Journal of Photochemistry & Photobiology, A: Chemistry 444 (2023) 114911

Contents lists available at ScienceDirect

Journal of Photochemistry & Photobiology, A: Chemistry

journal homepage: www.elsevier.com/locate/jphotochem

New fluorescent reporters capable of Ultra-sensitively detecting trinitrotoluene on surfaces: A proof-of-concept for finding hidden nitroaromatics in the workroom

Andrea Revilla-Cuesta, Irene Abajo-Cuadrado, María Medrano, Mateo M. Salgado, Giuditta Pecori, Teresa Rodríguez, Carla Hernando-Muñoz, José García-Calvo, Julia Arcos, Tomás Torroba *

Department of Chemistry, Faculty of Science, University of Burgos, 09001 Burgos, Spain

ARTICLE INFO

Keywords:
2,4,6-Trinitrotoluene
Improvised explosive devices
Chemical sensors
Fluorescent materials
Chemical tests
Swab alternatives

ABSTRACT

We describe the proof of concept of a portable testing setup for the detection of trinitrotoluene (TNT), a common component in hidden explosive devices. The system allows for field-testing and generation of real-time results to test for TNT traces in surfaces by simply using a filter paper and a fluorescent reporter. In this way, the controlled trapping and detection of the analyte by a chemical sensor gives reliable results at extremely low concentrations of TNT on surfaces under real life conditions suitable for daily use in ordinary sampling for example at airlines luggage storage or sport locker rooms. The reported fluorescent methodology is very sensitive and selective, allowing for the trapping and detection of TNT by a fluorescent reporter to give reliable results at very low concentrations. As a complement, we report the preparation of a modified Sylgard film that is useful under real conditions for qualitative fluorescent detection of hidden traces of TNT on surfaces or fingers by a swab method. The combination of quantitative and qualitative detection of TNT traces on surfaces constitutes a comprehensive new method for the detection of hidden nitroaromatic explosives in the workplace.

1. Introduction

A major threat in modern society is constituted by the so-called improvised explosive devices (IEDs). [1–6] The explosives contained in IEDs were commonly used in war scenarios but some years ago they were also used in situations of everyday life, therefore constituting a threat in the lives of countless people. Methods for the quick detection of explosive devices are needed before they cause damage, but there are very few methods for the detection of some explosives used in IEDs. [7–11] Indeed, the most advanced spectroscopy devices are very sensitive and selective to identify the chemicals used in IEDs, but they are typically too heavy for portable devices and too much expensive for widespread use. [12] The cheap technology of the cotton swab [13] requires physical access to the substance that might be hidden or not easily accessible. There is a long tradition in the use of animals in the detection of explosives, particularly trained dogs [14] but training and maintaining animals makes the method quite expensive. Electronic noses, made up of artificial sensor arrays, constitute a significant solution to replace the natural senses [15–16] for reliable monitorization of diverse environments. Appropriate portable devices for explosives used in the preparation of IEDs should alert to the presence of explosives within minutes. [17] Common methods for explosives containing nitro groups, such as trinitrotoluene (TNT) in air are known. [18] In solution, some turn-on fluorescent methods for their detection, including our contribution to the field [19] and from other groups [20–25] have been developed, but for the detection of TNT, the most common methods are based on fluorescence quenching [26–37] and selected biosensing methods, [38–40] with very few specially dedicated methodologies.

Abbreviations: IED, improvised explosive devices; TNT, trinitrotoluene; TNB, trinitrobenzene; DNT, 2,4-dinitrotoluene; NB, nitrobenzene; TATP, triacetone triperoxide; HMTD, hexamethylene triperoxide diamine; AIE, aggregation-induced emission; PDMS, polydimethylsiloxane; LOD, limit of detection; MCH, methylcyclohexane; m-CPBA, *meta*-chloroperbenzoic acid; IR, infrared; NMR, nuclear magnetic resonance; HRMS, high resolution mass spectrometry; MALDI, matrix-assisted laser desorption/ionization; ESI, electrospray ionization; UV–Vis, ultraviolet–visible; FL, fluorescence; Ø, quantum yield, τ, lifetime.

* Corresponding author.
E-mail address: ttorroba@ubu.es (T. Torroba).

https://doi.org/10.1016/j.jphotochem.2023.114911
Received 29 March 2023; Received in revised form 24 May 2023; Accepted 4 June 2023
Available online 8 June 2023

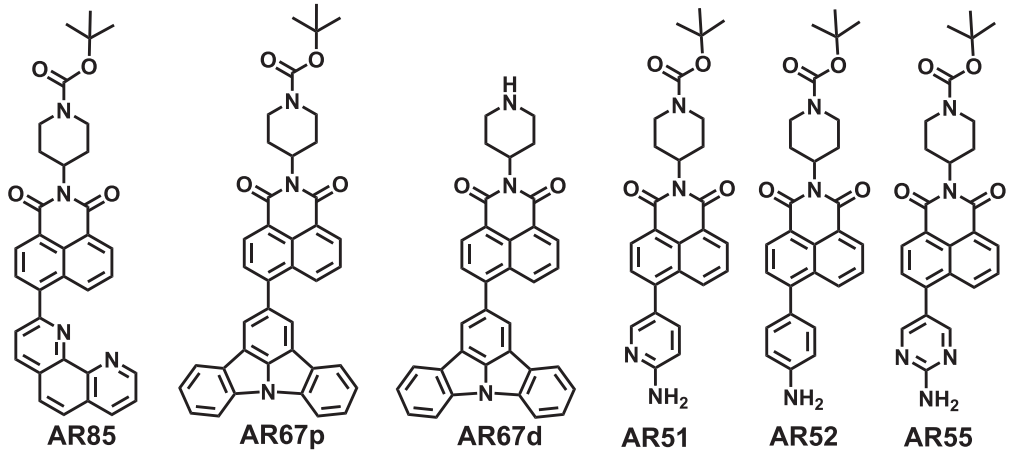

Fig. 1. Structure of chemical probes used for the study.

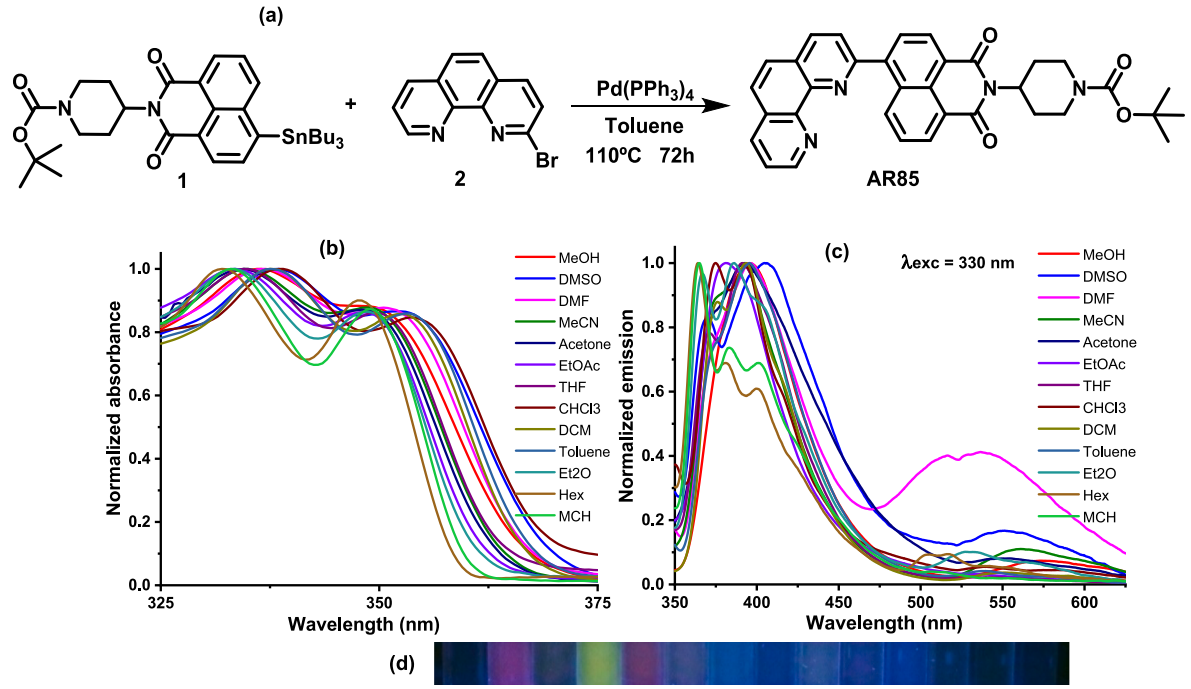

Fig. 2. (a) Synthesis of AR85, (b) normalized absorbance curves and (c) fluorescence emission curves in several solvents, (d) image of the fluorescence of AR85 solutions under UV light, 366 nm, AR85 10 μM in [1] H_2O, [2] MeOH, [3] DMSO, [4] DMF, [5] MeCN, [6] Acetone, [7] EtOAc, [8] THF, [9] $CHCl_3$, [10] CH_2Cl_2, [11] Toluene, [12] Et_2O, [13] Hexane and [14] MCH.

[41–42] Analytical methods for the detection of TNT in different scenarios must be selective for nitroaromatics, appropriate for immediate analysis and safe sampling by a qualified operator. They are expected to have very low limits of detection and high selectivity, in this way they can detect explosives in confined public places to prevent explosions and further damage. [43] Trace detection of TNT traces by fluorometric methods continues to be an attractive approach for the development of chemical sensors for hidden explosive devices. [44] We have some previous experience in fluorogenic sensors for the selective detection of explosive oxidants [45–48] This time, we looked for new fluorescent dyes in which a stacking event could modulate aggregation-induced emission (AIE) characteristics of dyes for the detection of nitroaromatic species. Naphthalimides are known to have AIE effects, [49–51] and some of them have been used for detection of trinitrophenol, an environmental contaminant and potential explosive. [52–53] We selected a collection of new naphthalimide structures with some classic donor or accepting groups in their structures, with the aim to maximize the expected interactions with classic nitroaromatic derivatives, and tested them for TNT detection, in this way we arrived to a new naphthalimide dye with optimum features for the selective and ultrasensitive detection of traces of TNT on surfaces and a new material for solvent-free fast detection of TNT on surfaces. In this way, the

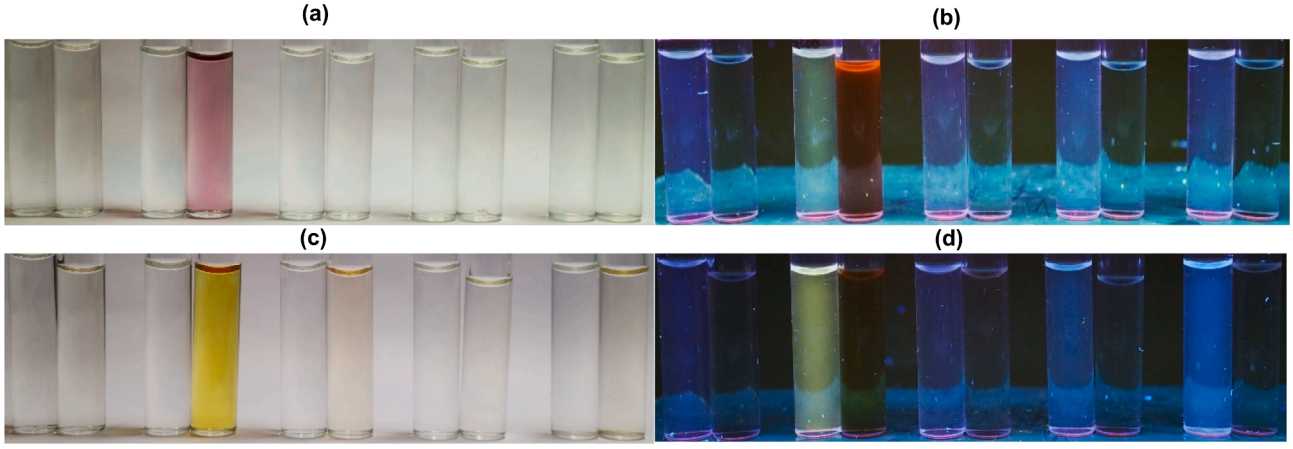

Fig. 3. AR85 10 μM (left vial of each pair) and AR85 10 μM with 7 mg of TNT (right vial of each pair) in (a-b), or TNB (c-d), from left to right, MeOH, DMF, MeCN, AcOEt, THF under visible light (a, c) and under UV light, 366 nm (b, d).

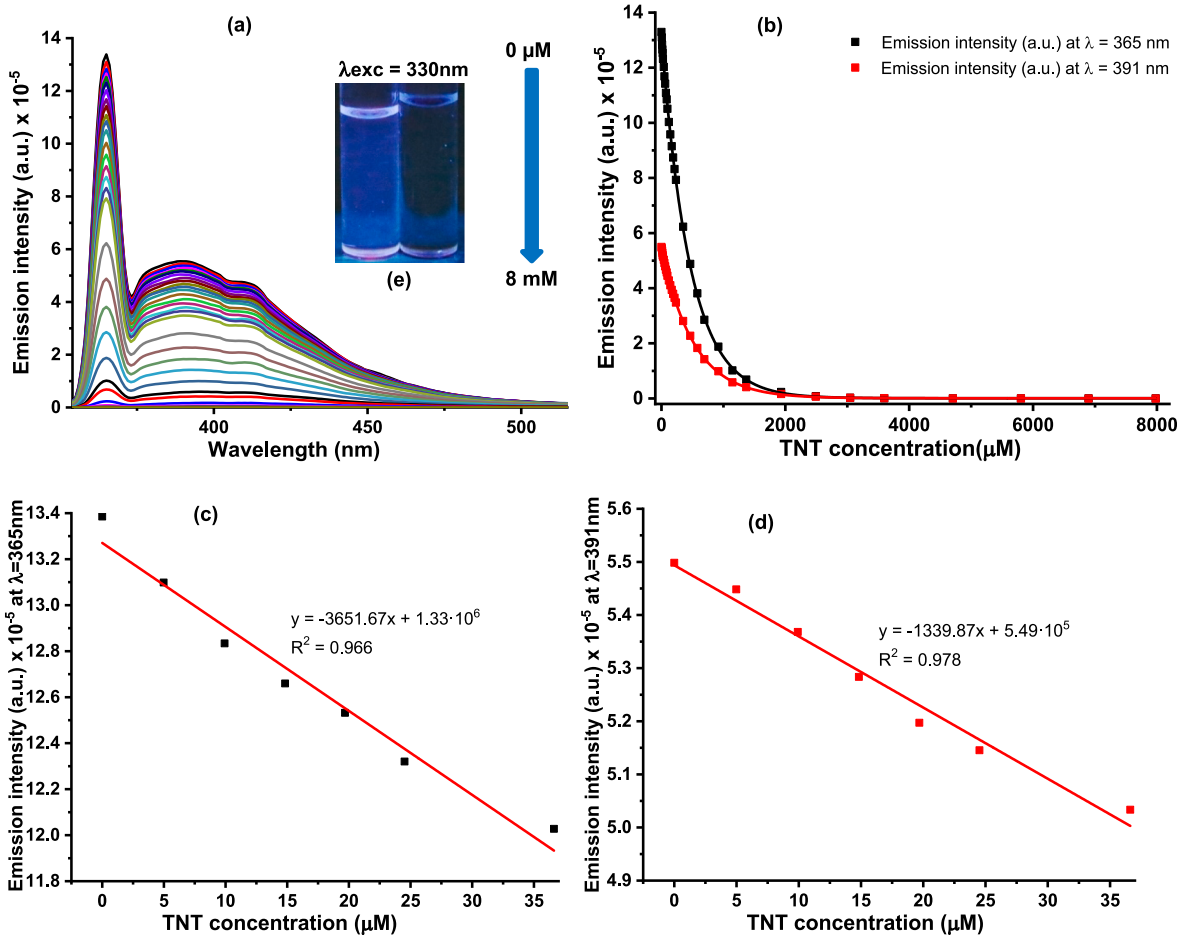

Fig. 4. Titration curves (a) and fluorescent profile at 365 and 391 nm (b), calibration for the limit of detection using emission values at 365 nm (c) and calibration for the limit of detection using emission values at 391 nm (d) of an AR85 solution, 2.5 μM in toluene, under increasing concentrations of TNT. Inset (e): A vial solution before and after the titration under UV light, 366 nm.

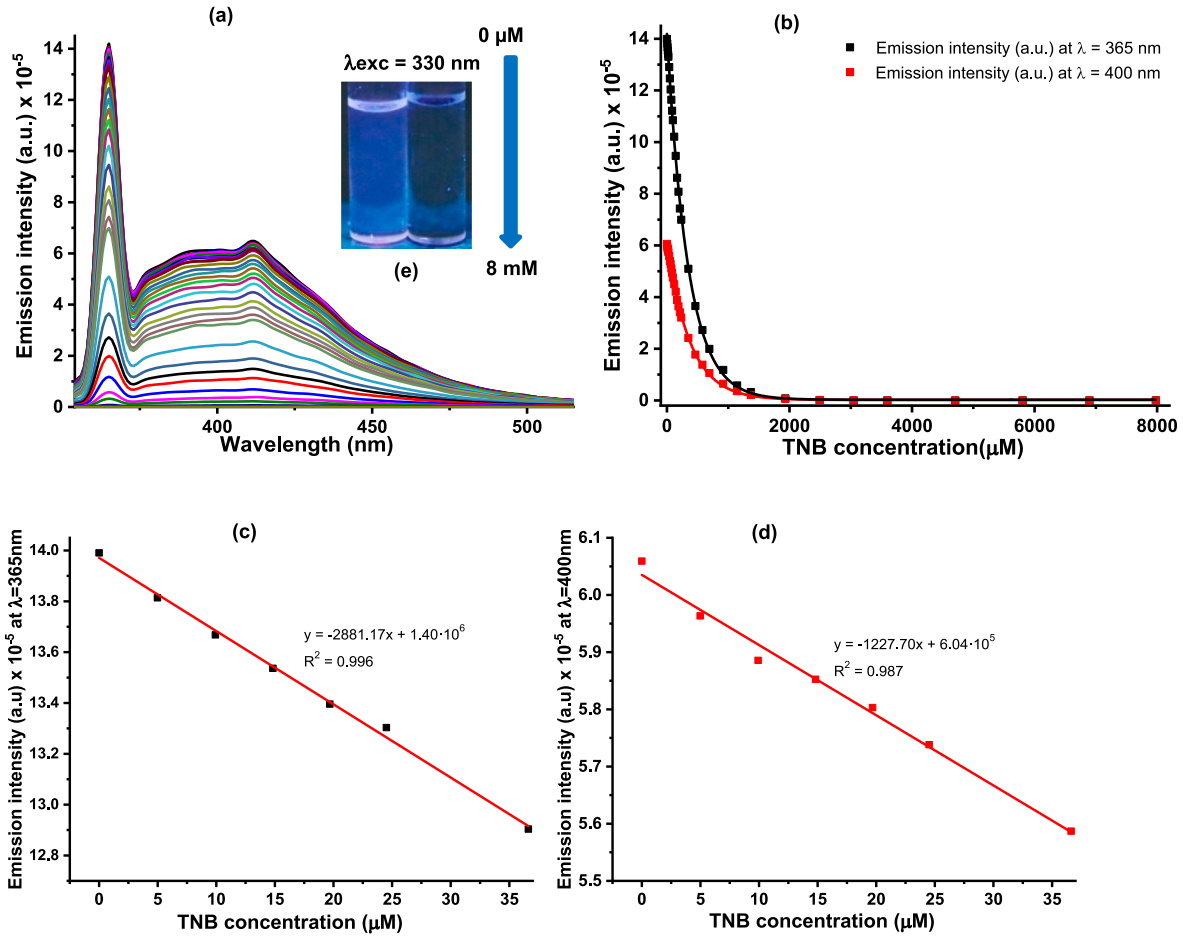

Fig. 5. Titration curves (a) and fluorescent profiles at 365 and 400 nm (b), calibration for the limit of detection using emission values at 365 nm (c) and calibration for the limit of detection using emission values at 400 nm (d) of an AR85 solution, 2.5 μM in toluene, under increasing concentrations of TNB. Inset (e): A vial solution before and after the titration under UV light, 366 nm.

materials functioned as useful alternatives to known chemical tracking systems of traces of TNT. The results of the study are presented here.

2. Results and discussion

We synthesized a number of fluorogenic probes that were tested for several types of analytes. The synthesis was performed by using carbon–carbon coupling chemistry, following previous experiences in developing fluorogenic probes by the group. [54–62] The new fluorogenic probes are shown in the Fig. 1. The selectivity of each fluorogenic probe against the most important nitroaromatic derivatives was addressed in organic-aqueous solvents, with the aim to select the best candidates for explosives. With the new fluorogenic probes we performed a complete characterization and a battery of preliminary tests about selectivity and sensitivity with target explosives and several expected interferents. The sensitivity of the collection of fluorogenic probes was checked in the presence of trinitrotoluene, TNT, trinitrobenzene, TNB, and their taggants, 2,4-dinitrotoluene and nitrobenzene. We prepared an experimental design for this part of the work that was applied to all fluorescent probes. Then, the sensitivity of selected solid supported naphthalimides was studied in the presence of traces of TNT, so the fluorogenic material could be capable of discriminate the presence of the most important explosive, TNT. Having a previous experience in modified materials, [45–46,48,56,63–64] we performed additional experiments by supporting a fluorescent probe on polydimethylsiloxane (PDMS) to study a quick positive detection that could be confirmed under careful titration with the best probe in solution.

The synthesis of AR85 was performed by Stille coupling between equimolecular amounts of *N*-(1-Boc-piperidin-4-yl)-4-(tributylstannyl) naphthalene-1,8-dicarboxylmonoimide 1 and 2-bromo-1,10-phenanthroline 2 under $Pd(PPh_3)_4$ catalysis in refluxing toluene for 72 h. Work-up and column chromatography afforded AR85 as a yellowish solid in 85 % yield (Fig. 2).

Compound AR85 was faintly fluorescent, very solvatochromic, in several solvents (Fig. 2). In preliminary tests, AR85 resulted to be insensitive to the presence of water in mixtures of THF and water, insensitive to pH values between 3 and 10 and insensitive to almost all common anions and cations. In tests with common oxidants or reducing agents it showed to be sensitive to the presence of TNB and TNT, so a search for the best solvent for their detection was performed (Fig. 3).

Albeit DMF was a suitable solvent for TNT/TNB titrations, the almost instant interaction of the solvent with the analytes hindered the fluorescent detection process. [65] After some Lambert-Beer tests we selected a working concentration of 2.5 μM for all experiments (Supporting Information pp. S14 and S28-S30) and after several titration experiments, we selected toluene as the solvent showing the highest sensitivity of AR85 to nitroaromatics (Supp. Info. pp. S15-S28 and S30-S32). Kinetic experiments showed that the emission intensity decreased

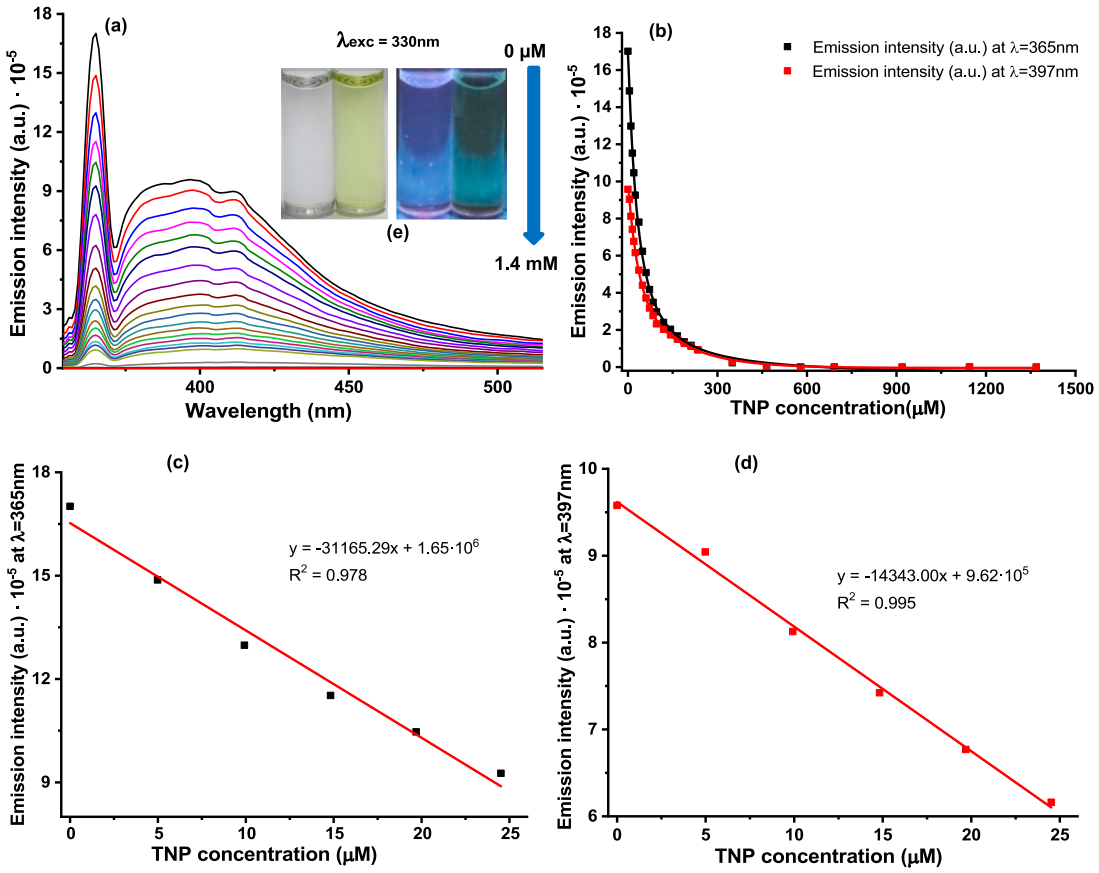

Fig. 6. Titration curves (a) and fluorescent profiles at 365 and 397 nm (b), calibration for the limit of detection using emission values at 365 nm (c) and calibration for the limit of detection using emission values at 397 nm (d) of an AR85 solution, 2.5 μM in toluene + 5%DMSO, under increasing concentrations of TNP. Inset (e): vials before and after TNP titration under visible light and 366 nm UV light, the yellow-green color of TNP is clearly visible in both images. (For interpretation of the references to color in this figure legend, the reader is referred to the web version of this article.)

immediately after adding TNT/TNB to AR85 solutions and the decreased intensity remained stable for long periods of time in all studied solvents (Supp. Info. pp. S15-S25). Therefore, we performed accurate titrations of a solution of AR85 (2.5 μM) in toluene with increasing amounts of TNT by successive additions from a concentrated solution in the same solvent, fluorescent measurements were carried out immediately after the addition of TNT at λ_{exc} = 330 nm, λ_{em} = 365 nm and 391 nm, and the fluorescence changes were registered at 25 °C. In addition, the blank (sample only containing probe) was measured three times. The titration curves and titration profile for TNT showed in Fig. 4 were obtained.

We calculated the limit of detection, LOD, from the initial titration plot values by IUPAC-consistent methods. [66] The limit of detection (LOD) by using emission values at 365 nm was calculated by a linear regression + false positive and negative values, [67] by: (1) Adjusting to a mean square linear regression, (2) removing the "outliers", understanding them as points that are significantly different from the rest, within a 95% of probability, (3) adjusting to a linear regression and checking that the slope is significantly different from 0 (95%), P-Value > 0.05, (4) calculating the LOD when the probability of false positive (α) and false negative (β) is equal or inferior to 5%, which is performed by the software "R" to provide the fitting and delivering of the results. [68] This method allowed to obtain a LOD = 1.87 nM or 0.42 ng × mL^{-1} of TNT. The LOD calculated by using emission values at 391 nm by a linear regression + false positive and negative values and using the R software, as in previous calculation, allowed to obtain a similar LOD = 1.87 nM, showing that both wavelength values decrease uniformly in the presence of TNT. For the simplicity of the method, this LOD competes in accuracy with alternative, much more complicate methodologies. [69] Similarly, titrations of AR85 solutions, 2.5 μM in toluene, with increasing amounts of TNB at λ_{exc} = 330 nm, λ_{em} = 365 nm and 400 nm, at 25 °C gave the titration curves and titration profile for TNB showed in Fig. 5.

We calculated the limit of detection, LOD, from the titration plot values by IUPAC-consistent methods. [66] In this case, we calculated the LOD within the values measured (different than 0) by adjusting the initial values to a mean square linear regression and using the R program. [67–68] In this way, linear regression at low concentrations of TNB led to a LOD = 1.88 nM or 0.40 ng × mL^{-1} of TNB, calculated by using emission values at 365 nm. Again, the LOD calculated by using emission values at 400 nm calculated by the same methodology gave a similar LOD = 1.89 nM, showing that both wavelength values decrease uniformly in the presence of TNB.

We have previously stated that some naphthalimides have been used for detection of trinitrophenol (TNP), an environmental contaminant and potential explosive, [52–53] therefore we wanted to study the performance of the fluorescent probe in the detection of TNP, in comparison to the detection of TNT and TNB. As in previous cases, a study of the behaviour of AR85 in the presence of excess TNP in different solvents was performed (Supp. Info. pp. S32-S33). TNP was soluble in MeOH, DMSO, acetone and THF but it was not completely soluble in DCM or $CHCl_3$ or toluene, but it was soluble in toluene with 5% v/v of DMSO. To keep the titration conditions as similar as possible to those previously carried out with TNT and TNB, the titration with TNP was performed in

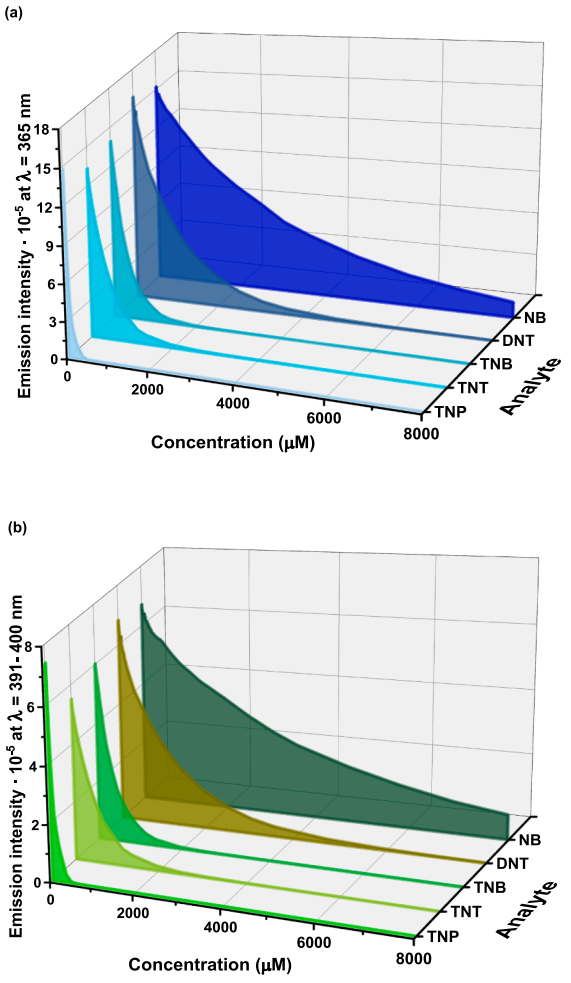

Fig. 7. Variation of the emission intensity of a 2.5 μM solution of AR85 in toluene versus increasing concentrations of TNP, TNT, TNB, DNT and NB at 365 nm (a) and 391–400 nm (b).

a mixture of toluene + 5% DMSO. In this way, titrations of AR85 solutions, 2.5 μM in toluene + 5% DMSO, with increasing amounts of TNP at λ_{exc} = 330 nm, λ_{em} = 365 nm and 397 nm, at 25 °C, gave the titration curves and titration profile for TNP showed in Fig. 6.

We calculated the limit of detection, LOD, from the titration plot values by IUPAC-consistent methods. [66] In this case, we calculated the LOD within the values measured (different than 0) by adjusting the initial values to a mean square linear regression and using the R program. [67–68] In this way, linear regression at low concentrations of TNP, by using the emission values at 365 nm, gave a LOD = 2.16 nM or 0.49 ng × mL^{-1} of TNP. Again, the LOD calculated by using emission values at 397 nm, calculated by the same methodology, gave a similar LOD = 2.19 nM, showing that both wavelength values decrease uniformly in the presence of TNP, as it happened in previous examples. The obtained LODs compete favorably with those obtained in previously known examples. [52–53] Then we were curious about the possibility of detecting one explosive taggant, such as 2,4-dinitrotoluene (DNT), [70] or the most common nitrobenzene (NB). In both cases we got related titration curves and titration profiles (Supp. Info. pp. S36-S39) but the LODs were lower than in previous cases (2.16 nM for DNT and NB). The simultaneous plotting of the variation of the emission intensity of a 2.5 μM solution of AR85 in toluene versus the increasing concentration of the 5 studied analytes showed a higher selectivity in the response of AR85 to the most nitrated derivatives (Fig. 7) that depended on the number of the nitro groups and the phenol moiety to exert an increased response of fluorescent quenching at very low concentrations of the analyte. Albeit the fastest decrease of the fluorescence of AR85 happened in the presence of increasing amounts of TNP, the lowest LOD was found in the presence of TNT.

To understand the interaction between AR85 and TNT, we performed an NMR titration in deuterated benzene. Initially, ^{1}H NMR spectra of TNT (10 mg in 0.5 mL in C_6D_6) and AR85 (4 mg in 0.5 mL in C_6D_6) were performed as references. After this, increasing amounts of TNT were added to the NMR tube corresponding to AR85 to carry out the titration (Fig. 8).

An expanded region between 7.45 and 6.85 ppm showed the interaction of AR85 and TNT was seen as a complex coupling and simultaneous shift of the triplet at 7.03 ppm and sifting of the signals at 6.88 and 7.33 ppm, by apparent π-π stacking interaction between TNT and the phenanthroline moiety of AR85. The extreme sensitivity of AR85 to the presence of TNT may have practical applications. One of the most used methods for the detection of TNT traces consists of a swab passed through a surface to get hidden traces of solid TNT which is then subjected to analytical methods. As an alternative to these methodologies we performed a controlled experiment to test AR85 as a powerful probe for TNT. Thus, increasing amounts of TNT (every one calculated to be dissolved in a final volume of 2.5 mL to afford the appropriate concentrations for the titrations shown in Fig. 6) were deposited on a watch glass and left to evaporate to dryness. A fragment (1 cm × 0.5 cm) of filter paper was slid over the watch glass to capture the TNT traces. Each piece of filter paper was then placed in a topaz vial to which 3 mL of MeOH were added. Every vial was then sonicated in an ultrasonic bath for a period of 5 min. After this, the filter paper was removed from the vial and the solvent was evaporated until complete dryness under nitrogen stream and gentle warming in an air stream. Finally, the probe in toluene and more toluene were added to get a final concentration of AR85, 2.5 μM in a final volume of 2.5 mL, and the fluorescence emission spectra were measured, as shown in Fig. 9.

The titration profile for TNT showed on Fig. 9 was obtained. Again, we calculated the LOD within the values measured (different than 0) by adjusting the initial values to a mean square linear regression and using the R program. [67–68] Because of the large fluctuations in the spectra, a careful selection of representative values and outliers to be removed was performed with the help of the R program. By using the values at 365 nm, the LOD calculated by the same methodology gave LOD = 17.31 μM or 3.93 ng·mL^{-1} of TNT. Analogously, linear regression at low concentrations of TNT, calculated by using emission values at 391 nm, led to a LOD = 17.24 nM or 3.91 ng × mL^{-1} of TNT, showing that the detection of TNT residual on surfaces by using a simple filter paper as swab was performed quantitatively with good reliability and accuracy under real-life conditions. Weighing all steps, we calculated that in the cases of the lowest concentrations (up to around 700 μM), the swap collected almost 100% of TNT, and within the highest concentrations (from 700 μM to the end of the titration) about 90%, thus supporting the feasibility of the detection process. The large fluctuations observed in the titration spectra of Fig. 9, with respect to clean spectra observed in Fig. 4, could be produced by small impurities gained during the process, dust, solvent residuals, etc., therefore a careful study of interferents was performed to understand the implications that should have in the measurements of TNT detection. The effects that the presence of cations, anions, redox agents, other explosive, etc., may have on the TNT determination of AR85 have been studied and the results are shown in Fig. 10 as normalized emission intensity values, by using AR85 maximum emission intensity as the reference. We performed those tests by dissolving AR85 in THF (2.5 μM) as a general solvent (so the comparison with the tests in toluene is only approximate because many of

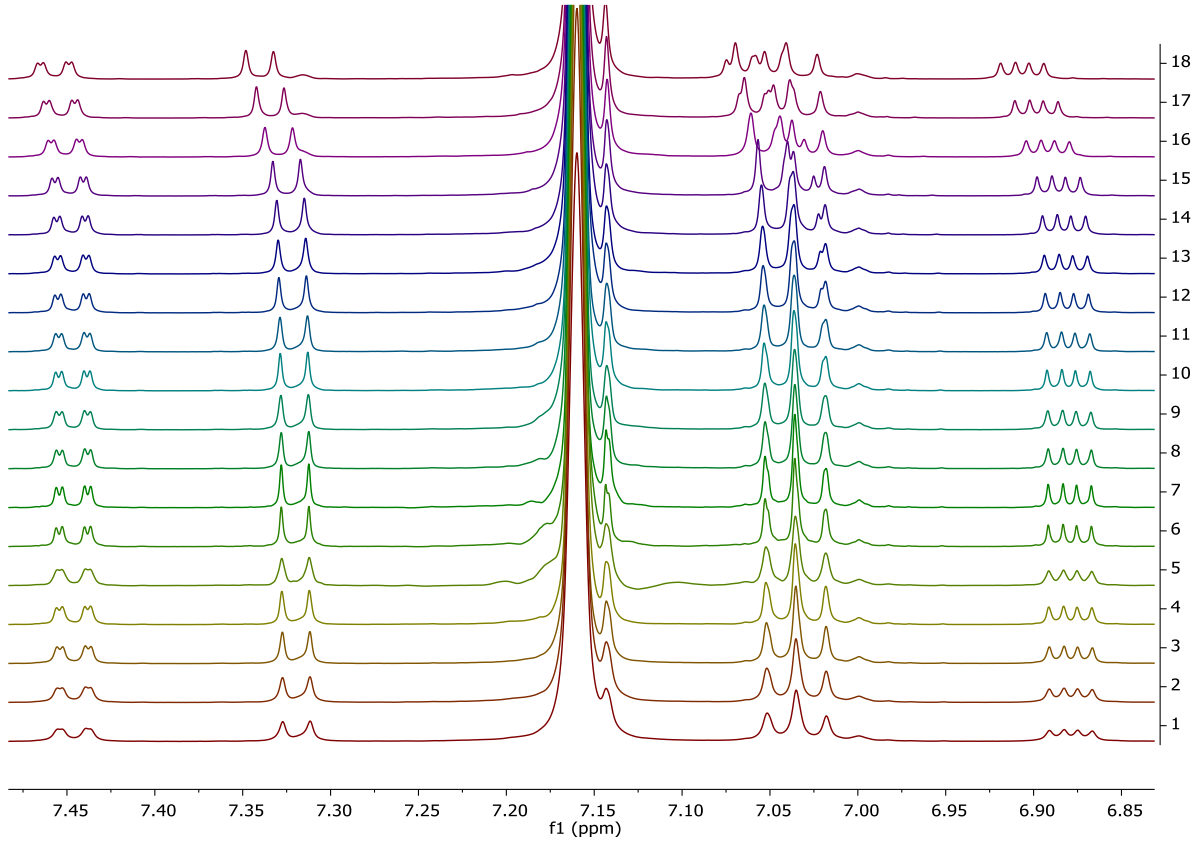

Fig. 8. Expanded region of NMR titration of AR85 (4 mg in 0.5 mL in C_6D_6) with increasing amounts of TNT (1) pristine AR85, (2) + 5 μg TNT, total: 5 μg, (3) + 5 μg, total: 10 μg, (4) + 5 μg, total: 15 μg, (5) + 5 μg, total: 20 μg, (6) + 10 μg, total: 30 μg, (7) + 10 μg, total: 40 μg, (8) + 20 μg, total: 60 μg, (9) + 30 μg, total: 90 μg, (10) + 60 μg, total: 150 μg, (11) + 150 μg, total: 300 μg, (12) + 200 μg, total: 500 μg, (13) + 300 μg, total: 800 μg, (14) + 600 μg, total: 1400 μg, (15) + 1800 μg, total: 3200 μg, (16) + 3600 μg, total: 6800 μg, (17) + 3600 μg, total: 10400 μg, (18) + 5400 μg, total: 15800 μg.

the interferents are not soluble in toluene), then adding TNT (8 μL 5 × 10^{-3} M solution in MeOH, 8 eq), and then adding to each sample vial Ag^{+}, Ni^{2+}, Sn^{2+}, Cd^{2+}, Zn^{2+}, Pb^{2+}, Cu^{2+}, Fe^{3+}, Sc^{3+}, Al^{3+}, Hg^{2+}, Au^{3+}, Co^{2+}, Pd^{2+}, Ir^{3+}, Cu^{+}, Ru^{3+}, Pt^{2+}, F^{-}, Cl^{-}, Br^{-}, I^{-}, BzO^{-}, NO_3^{-}, NO_2^{-}, $H_2PO_4^{-}$, HSO_4^{-}, AcO^{-}, CN^{-}, SCN^{-}, HCl, HNO_3, oxone, hydrazine, and H_2O_2 (8 μL 5 × 10^{-3} M solution in water, 8 eq), then TNB (8 μL 5 × 10^{-3} M solution in MeOH, 8 eq), and then *meta*-chloroperbenzoic acid (*m*-CPBA), triacetone triperoxide (TATP) and hexamethylene triperoxide diamine (HMTD) (2 mg as a solid) (Fig. 10).

Every time the mixture of solvents was modified, a reference solution of AR85 was used (experiments with redox agents and other explosives or oxidants). In all cases, a decrease in the intensity of the probe emission is observed after the addition of 8 equivalents of TNT. In most of the experiments, the intensity of the fluorescence emission did not change after the addition of 8 equivalents of common cations, anions, redox agents or other explosives in solution, except in three cases. In the presence of NO_3^{-} the fluorescence increased notably, but there was no effect of the presence of NO_2^{-}. There was a decrease in fluorescence in the presence of Au^{3+}, albeit it was not considered a common interferent. *m*-CPBA produced and enormous increase in fluorescence because of the oxidant nature of the reagent, but there was no effect of the presence of explosive oxidants such as TATP or HMTD. Nitrate anion can be found in explosive mixtures as ammonium nitrate; therefore, we performed a full titration study of AR85 and ammonium nitrate. We performed a previous study of solvents for the titration (Supp. Info. pp. S40) and concluded that to perform the titration in the closest conditions to previous examples, the mixture of toluene + 5% DMSO w/w was appropriate. Therefore, on a solution of AR85 (2.5 μM) in toluene + 5% DMSO, successive amounts of NH_4NO_3 from a concentrated solution in the same solvent were added, measurements were carried out immediately after the addition, λ_{exc} = 330 nm, λ_{em} = 365 nm/397 nm, and fluorescence changes were registered at 25 °C. Samples of the AR85 solution were taken before and after the titration and photographed under visible light and 366 nm UV light (Fig. 11).

We calculated the limit of detection, LOD, from the titration plot values by IUPAC-consistent methods. [66] In this case, as before, we calculated the LOD within the values measured (different than 0) by adjusting the initial values to a mean square linear regression and using the R program. [67–68] In this way, linear regression at low concentrations of TNP, by using the emission values at 365 nm, gave a LOD = 11.31 μM or 0.90 μg × mL^{-1}. Again, the LOD calculated by using emission values at 397 nm, calculated by the same methodology, gave a related LOD = 9.60 μM, much higher, in both cases, than in previous examples with nitrated explosives or taggants. Thus, the detection of ammonium nitrate, albeit in much higher amounts than nitrated explosives, may complement the usefulness of the fluorescent probe in the detection of traces of explosive substances. To complement this series, we then tested the effect of the other explosives in the swab methodology by performing the experiments in the presence of mixtures of TNT and another explosive or taggant in each case. Thus, increasing amounts of equimolecular amounts of TNT and another explosive or taggant (TATP, HMTD, TNB, NB, DNT, TNP, NH_4NO_3), calculated to give 0, 5, 10, 15 and 20 equivalents of each one when dissolved in 2.5 mL, were deposited on a watch glass, then a fragment of filter paper (1 × 0.5 cm)

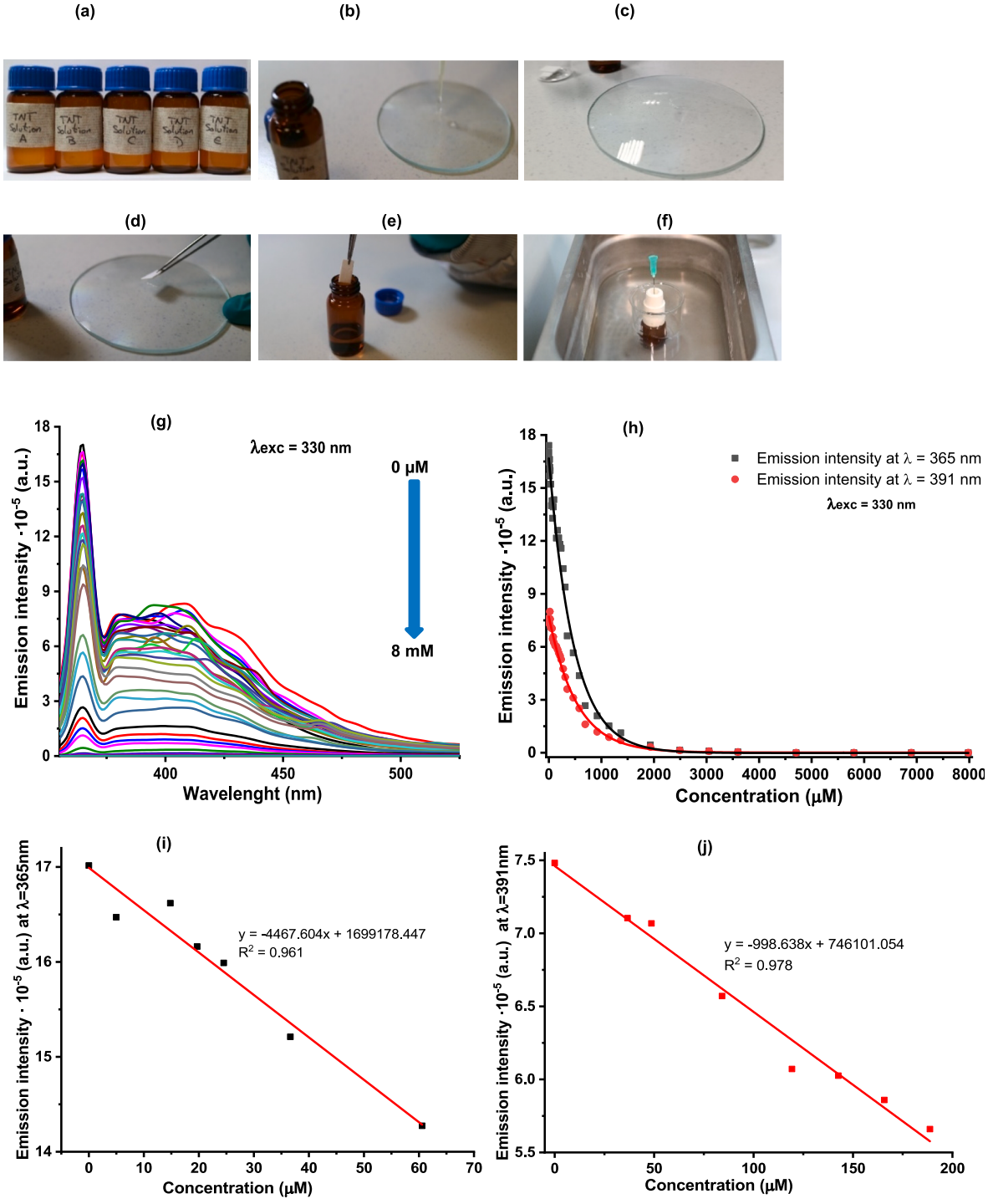

Fig. 9. (a) TNT solutions used in the experiment, (b) TNT deposition process on the watch glass, (c) TNT sample after the air-drying process of the solution, (d) capture of the TNT with a piece of filter paper, (e) Insertion of filter paper into a topaz vial, (f) sonication of the sample after removal of the filter paper, (g) Titration curves, (h) fluorescence profile at 365 and 391 nm, (i) calibration for the limit of detection using emission values at 365 nm and (j) calibration for the limit of detection using emission values at 391 nm of a 2.5 µM AR85 solution in toluene, in contact with increasing amounts of TNT collected on a paper filter, dissolved in 2.5 mL toluene, to give progressive TNT concentrations shown in the titration (λ_{exc} = 330 nm, T = 25 °C).

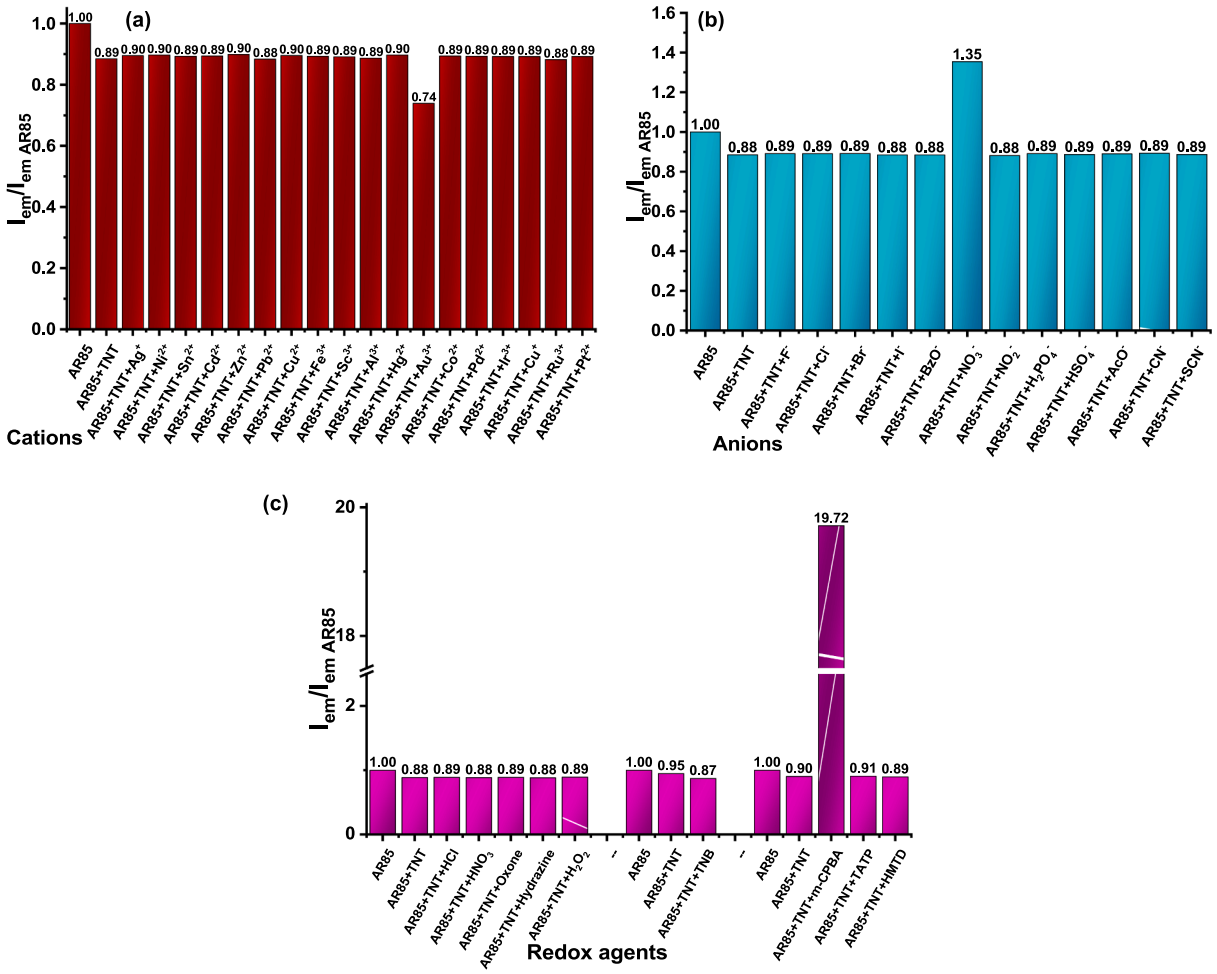

Fig. 10. Interference tests between AR85 and common cations (a), anions (b), acids, redox agents, and other explosives or oxidants (c), in normalized emission intensity graphs, using AR85 measurement as reference.

was slid over every one, placed in a topaz vial, and added of 3 mL MeOH. Then the vials were sonicated in an ultrasonic bath for 5 min, after that the paper fragments were removed, and the solvent evaporated under nitrogen stream and gentle warming in an air stream. Finally, 2.5 mL of AR85, 2.5 μM in toluene are added and the fluorescence emission spectra were measured. The fluorescence emission intensities corresponding to the measurements at 365 and 391 nm are shown Fig. 12.

Fig. 12 showed that the fluorescence values corresponding to TNT + TATP and TNT + HMTD were similar to the presence of TNT alone, because those explosives do not interfere with the determination of TNT (as observed in Fig. 10), as well as in the presence of the explosive taggants DNT and NB. The decrease in fluorescence in the case of the presence of TNT + TNP is remarkable because of the higher sensitivity of AR85 to TNP with respect to TNT. In the case of TNT + NH_4NO_3, the behavior is anomalous due to the contrary behavior of each species, a fluorescence emission decrease with TNT from low concentrations, and a fluorescence emission increase with NH_4NO_3 at high concentrations.

Looking for a large scope of the method by extending the procedure to environmental samples, we then tested the detection of TNT traces in water and sand. Thus, increasing amounts of TNT, calculated to give 0, 5, 10, 15 and 20 equivalents when dissolved in 2.5 mL, were added to 10 mL of filtered tap water samples, then the mixtures were extracted with toluene (3 × 10 mL), the organic fractions were collected and then evaporated under nitrogen flow and gentle warming under a warm air stream. Finally, 2.5 mL of AR85, 2.5 μM in toluene, were added and the fluorescence spectra were measured (Fig. 13). Analogously, increasing amounts of TNT, calculated to give 0, 5, 10, 15 and 20 equivalents when dissolved in 2.5 mL, were added to samples of 1 g sand (sea sand, washed, thin, grain size approx. 300–350 μm) placed in topaz vials, then 3 mL of MeOH were added and vials were sonicated in an ultrasonic bath for a period of 2 min. After that, the content was filtered, the solid was discarded and the solvent from the liquid phase was evaporated under nitrogen stream and gentle warming in an air stream. Finally, 2.5 mL of AR85, 2.5 μM in toluene, were added and the fluorescence emission spectra were measured. (Fig. 13).

From the detection tests carried out in water, we concluded that the sensitivity of AR85 probe to TNT in water remained intact, being able to detect the presence of TNT in very low amounts. On the other hand, from the detection tests carried out in sand, we concluded that the sensitivity of AR85 probe to TNT in sand was significantly affected. The probe was still capable of detecting low concentrations of TNT, but the fluorescence quenching was much lower than in the previous case, probably because retention of TNT on sand could give to incomplete extraction of TNT from the samples. Therefore, it is possible to perform a fair detection of TATP in water or sand, but sensitivity from water samples was much better than from sand samples.

To complete a real alternative to current swab methodologies, a quick TNT fluorescent detection should be required. AR85 was only

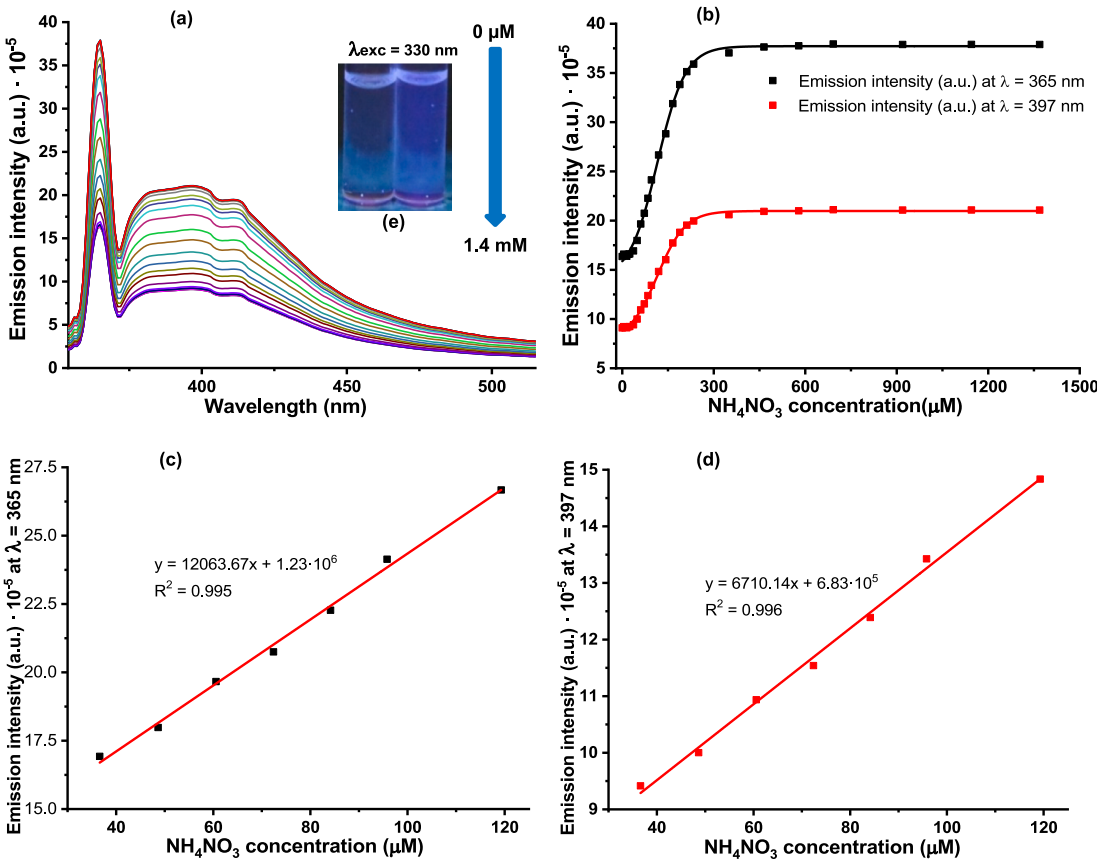

Fig. 11. Titration curves (a), fluorescence profiles at 365 and 397 nm (b), calibration for the limit of detection using emission values at 365 nm (c) and calibration for the limit of detection using emission values at 397 nm (d) of a 2.5 μM AR85 solution in toluene + 5% DMSO, under increasing concentrations of ammonium nitrate. Inset (e): A vial solution before and after the titration under UV light, 366 nm.

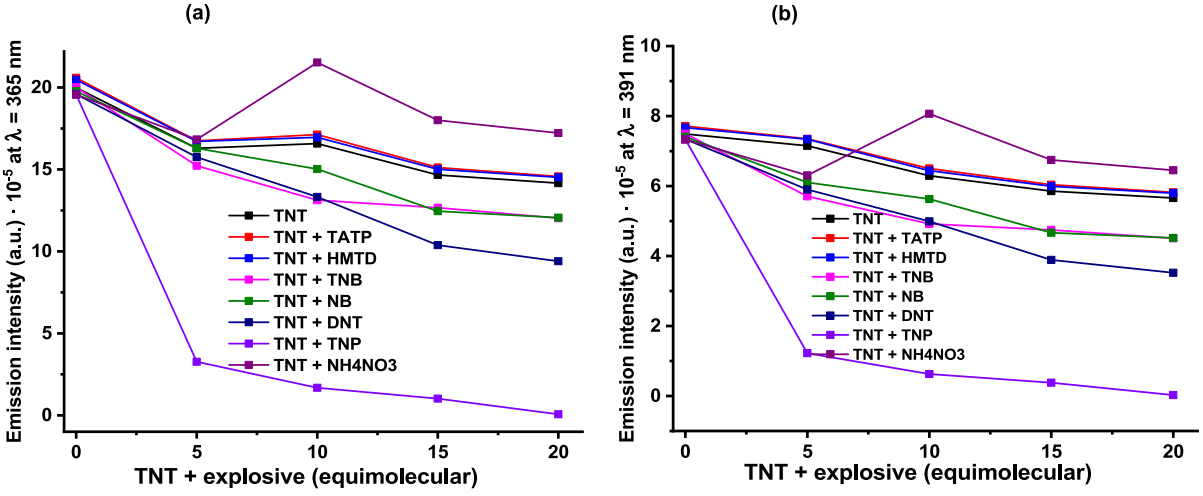

Fig. 12. Fluorescence profile at 365 nm (a) and 391 nm (b) of a 2.5 μM AR85 solution in toluene, in the presence of increasing amounts of TNT, TNT + TATP, TNT + HMTD, TNT + NB, TNT + DNT, TNT + TNP and TNT + NH_4NO_3 in 0, 5, 10, 15 and 20 equivalents when collected on a filter paper and dissolved in 2.5 mL MeOH.

faintly fluorescent for naked eye clear detection therefore we searched between the collection of fluorescent probes of Fig. 1. GP02, MMH2, MMH3 and CH07 were extremely fluorescent compounds in common organic solvents of intermediate polarity but they did not show any characteristic sensitivity to common cations, anions, oxidant o reducing compounds in organic solvents. Therefore, we selected the most representative of them, GP02, a very fluorescent compound in all common solvents except methanol and water, to prepare a solid material for solid TNT detection based on ability of TNT of quenching fluorescence. The synthetic process is shown in Fig. 14. The synthesis of GP2 was performed by Suzuki coupling between equimolecular amounts of *N*-(1-Boc-piperidin-4-yl)-4-bromonaphthalene-1,8-dicarboxylmonoimide **3** and 2-(4,4,5,5-tetramethyl-1,3,2-dioxaborolan-2-yl)indolo[3,2,1-jk] carbazole **4** under $Pd(PPh_3)_4$ catalysis in refluxing toluene/butanol/water 4:1:2 v/v for 24 h. Work-up and column chromatography afforded GP02 as a yellowish solid in 86 % yield (Fig. 14). Deprotection of GP2 by

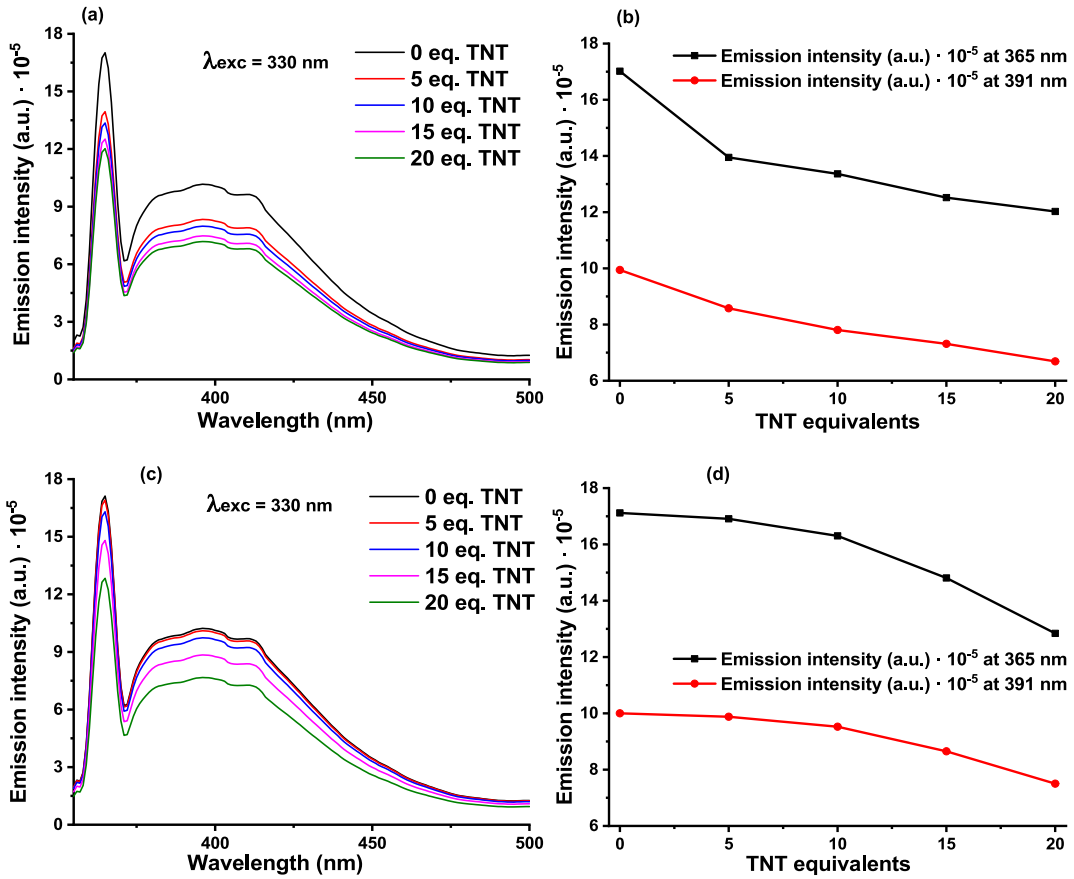

Fig. 13. Emission intensity spectra (a) and fluorescence profiles (b) at 365 and 391 nm of a 2.5 μM AR85 solution in toluene, in contact with increasing amounts of TNT collected from filtered tap water, in amounts that dissolved in 2.5 mL solvent gave 0, 5, 10, 15 and 20 equivalents. Emission intensity spectra (c) and fluorescence profiles (d) at 365 and 391 nm of a 2.5 μM AR85 solution in toluene, in contact with increasing amounts of TNT collected from sand in amounts that dissolved in 2.5 mL gave 0, 5, 10, 15 and 20 equivalents.

trifluoroacetic acid in chloroform gave quantitatively GP3, a very fluorescent and solvatochromic compound with the same optical characteristics of GP2 (Fig. 14). Reaction of GP03 with equimolecular amounts of triethoxy(3-isocyanatopropyl)silane **5** in chloroform at room temperature overnight gave the silylated derivative AR67-Si which was immediately subjected to reaction in toluene with Sylgard-184 (Dow Corning), previously activated with piranha and KOH solutions, [71] to get surface modified AR67@Sylgard-184.

The probe attached to the Sylgard-184 polymer surface, AR67@Sylgard-184, was used to perform contact tests in the presence of traces of solid TNT. In these tests, 0.5 mg of TNT was deposited and distributed evenly on a clean slide, a fragment of AR67@Sylgard-184 was picked up and dragged over the TNT covered area of the slide, and the changes were observed under UV light (366 nm) and by fluorescence measurements. In addition, 0.5 mg of TNT were diluted in 150 μL of MeOH, from them, 50 μL were taken and deposited on a finger covered with a clean, new glove, the finger was pressed on the surface of AR67@Sylgard-184 and the changes were observed under UV light (366 nm) and fluorescence measurements (Fig. 15). For comparison purposes, several tests in the presence of common solvents were also performed by placing 1 mL of solvent in a 12 mL topaz vial, AR67@Sylgard-184 was fixed to the inside of the vial stopper and the vial was warmed by air until evaporation of the solvent. The experiments showed a clear decrease in the fluorescent emission of the AR67@Sylgard-184 film in the presence of TNT traces from solid surfaces either on glass or finger, with an irregular pattern in the case of TNT on finger, which is very different of the very slight fluorescence variations in the presence of common solvents. The quantitative measurements showed also a clear quantitative decrease in the initial fluorescence of the film. Therefore, AR67@Sylgard-184 film is useful under real conditions for a quick qualitative detection of hidden TNT traces and, in combination with the quantitative detection of TNT traces on surfaces by AR85, in toluene solution, constitutes a comprehensive new method for the detection of hidden nitroaromatic explosives in the workplace. The system can be applied with little implementation of laboratory material at control points wherever it could be necessary.

As in the previous case, to extend the methodology to environmental samples, we also tested the detection of TNT traces in water and sand, this time by using AR67@Sylgard-184. Thus, increasing amounts of TNT (0, 0.10, 0.20, 0.30 and 0.40 mg) were added to 10 mL of filtered tap water samples, every mixture was extracted with toluene (3 × 10 mL) and the solvent evaporated under nitrogen stream and gentle warming (air stream). Then 0.5 mL of methanol were added to every sample, the solution was spread evenly on a clean slide and then dried by using a nitrogen flow. A fragment of AR67@Sylgard-184 film was grabbed with flat tweezers and dragged over the TNT-coated area of every slide. Fluorescence measurements before and after contacting the polymer with the TNT were performed in all cases studied. Fig. 16 represents the emission variations for every film fragment measured before and after the process. Photographs under UV light 366 nm of every film fragment before and after the process were also taken (Fig. 16). On the other hand, increasing amounts of TNT (0, 0.10, 0.20, 0.30 and 0.40 mg) were added

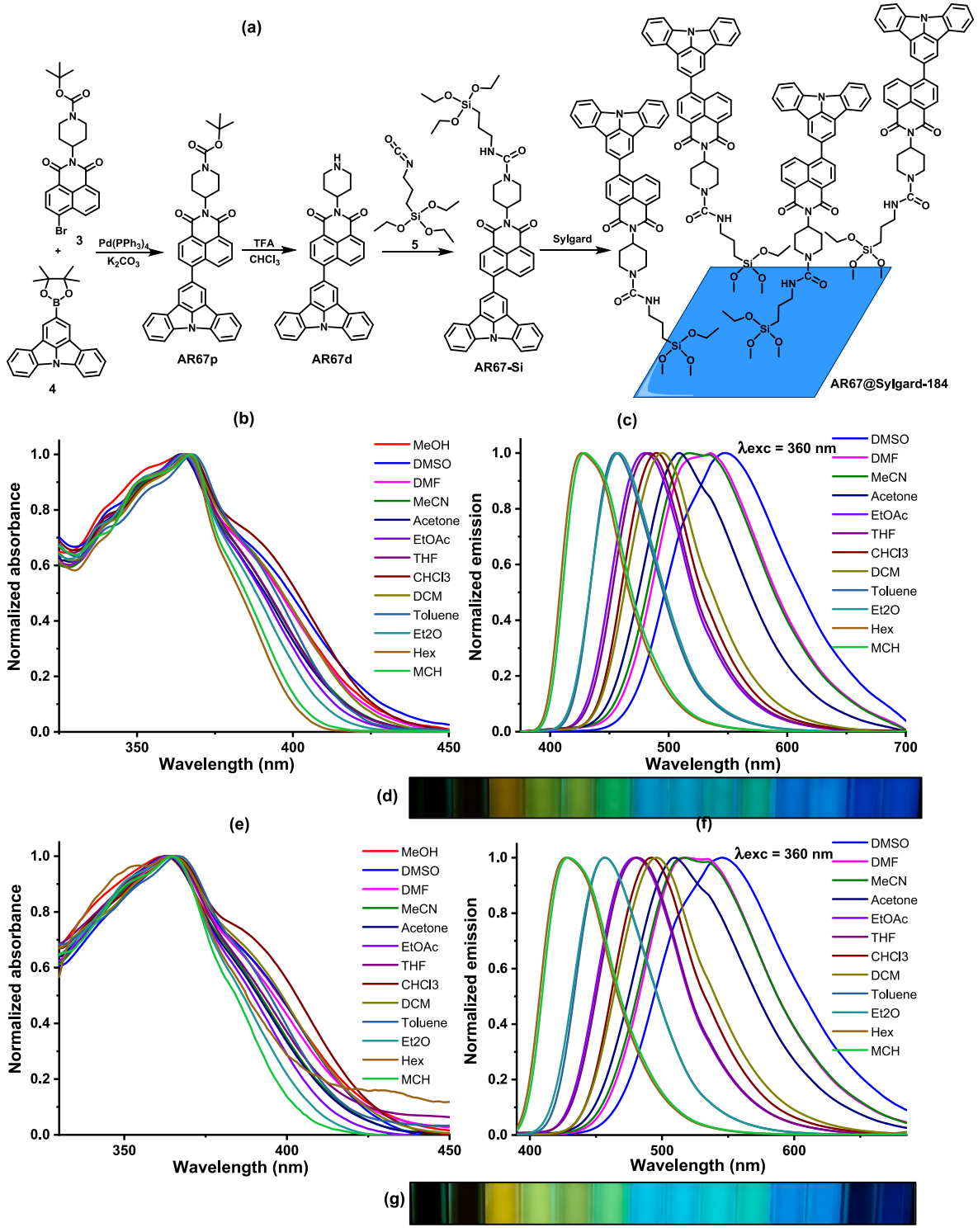

Fig. 14. (a) Synthesis of AR67p, AR67d and bonding to Sylgard-184, (b) normalized AR67p absorbance curves and (c) normalized AR67p fluorescence emission curves in several solvents, (d) image of the fluorescence of AR67p solutions under UV light, 366 nm, AR67p 10 μM in [1] H_2O, [2] MeOH, [3] DMSO, [4] DMF, [5] MeCN, [6] Acetone, [7] EtOAc, [8] THF, [9] $CHCl_3$, [10] CH_2Cl_2, [11] Toluene, [12] Et_2O, [13] Hexane and [14] MCH. (e) normalized AR67d absorbance curves and (f) normalized AR67d fluorescence emission curves in several solvents, (g) image of the fluorescence of AR67d solutions under UV light, 366 nm, AR67d 10 μM in the same list of solvents.

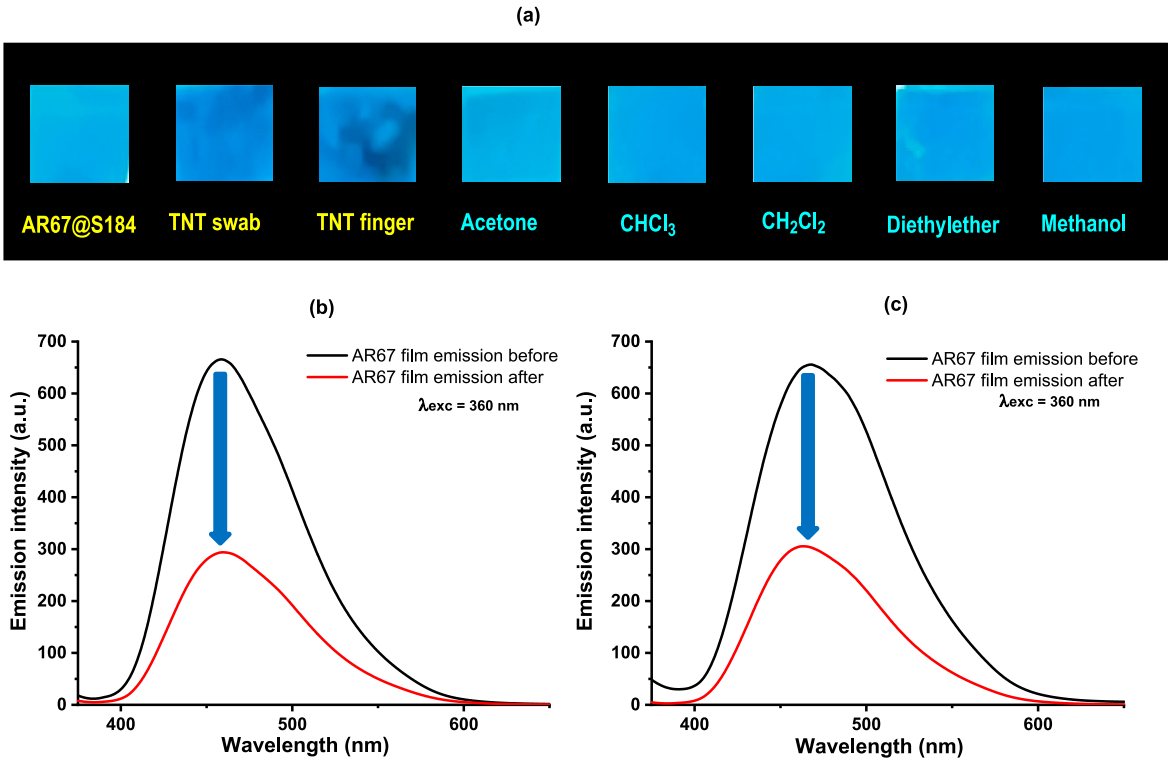

Fig. 15. (a) Photographs under UV light, 366 nm, of pristine AR67@Sylgard-184, and after contact with TNT on a surface as the film was used as a swab, TNT on finger after pressed over the film, vapors of acetone, chloroform, dichloromethane, diethylether and methanol. (b) Fluorescence curves of pristine AR67@Sylgard-184 and after contact with TNT on a surface as the film was used as a swab, or (c) after TNT on finger applied by pressing on the film.

to samples of 1 g sand, the samples were placed in topaz vials and 3 mL of MeOH added to each one and sonicated in an ultrasonic bath for 2 min. Then the samples were filtered, the solid discarded and the solvent evaporated in every case under nitrogen flow and gentle warming under air stream. Then 0.5 mL of methanol were added, the solution was spread evenly on a clean slide and then dried by using a nitrogen flow. A fragment of AR67@Sylgard-184 film was dragged over the TNT-coated area of the slide. Fluorescence measurements and photographs under UV light, 366 nm, before and after contacting the polymer with TNT were performed in all cases studied (Fig. 16).

We concluded that the sensitivity of AR67@Sylgard-184 to TNT under real conditions experiments from water and sand was still quite good in both cases, but specially for samples from water in which the sensitivity was fair for low amounts of TNT and at higher amounts the fluorescence quenching was remarkable. The retention of TNT by sand may affect also in this case to the sensitivity of the detection at low amounts of TNT. Therefore, the system is also suitable to perform a fair detection of TATP in water or sand.

To complete the series, for comparative purposes, we synthesized some new fluorescent naphthalimides by Suzuki reactions, similarly to the previous example. The synthetic process is shown in Fig. 16. The syntheses of AR51, AR52 and AR55 were performed by Suzuki couplings between equimolecular amounts of *N*-(1-Boc-piperidin-4-yl)-4-bromonaphthalene-1,8-dicarboxylmonoimide 3 and 4-(4,4,5,5-tetramethyl-1,3,2-dioxaborolan-2-yl)-1-arylamines 5–7 under $Pd(PPh_3)_4$ catalysis in refluxing toluene/butanol/water 4:1:2 v/v for 24 h. Work-up and column chromatography afforded the yellowish solids AR51, AR52 and AR55 in 83–90% yields (Fig. 17). Despite being very fluorescent and solvatochromic, these compounds did not show good sensing characteristics in the performed tests (Supp. Info. pp. S59-S60, S66-S67, S73-S74, and S78-S79).

3. Experimental methods

The selection of the appropriate dye for TNT detection consisted of an iterative process. First the synthesized compounds were fully characterized by physical and spectral methods, IR, $^{1}H/^{13}C$ NMR, HRMS (MALDI/ESI), UV–Vis, FL, Ø, τ. UV–Vis and Fluorescence measurements were performed in a series of 14 solvents from high to low polarity [1·H_2O, 2. MeOH, 3. DMSO, 4. DMF, 5. MeCN, 6. Acetone, 7. EtOAc, 8·THF, 9. $CHCl_3$, 10. CH_2Cl_2, 11. Toluene, 12. Et_2O, 13. Hexane, 14. Methylcyclohexane (MCH)]. Then, compounds were tested in solution for the sensitivity to low to high amounts of water (0 to 90% water, usually in THF), pH values (3.4 to 10.4), anions (11 representative anions: 1. F^-, 2. Cl^-, 3. Br^-, 4. I^-, 5. BzO^-, 6. NO^{3-}, 7. $H_2PO_4^-$, 8. HSO_4^-, 9. AcO^-, 10. CN^-, 11. SCN^-), cations (18 representative cations: 1. Ag^+, 2. Ni^{2+}, 3. Sn^{2+}, 4. Cd^{2+}, 5. Zn^{2+}, 6. Pb^{2+}, 7. Cu^{2+}, 8. Fe^{3+}, 9. Sc^{3+}, 10. Al^{3+}, 11. Hg^{2+}, 12. Au^{2+}, 13. Co^{2+}, 14. Pd^{2+}, 15. Ir^{3+}, 16. Cu^{+}, 17. Ru^{3+}, 18. Pt^{2+}), oxidizing and reducing agents in different solvents [(addition in water, series A: 1. HCl, 2. HNO_3, 3. Oxone, 4. Hydrazine, 5·H_2O_2) (addition in MeOH, series B: 1. *Meta*-chloroperbenzoic acid (m-CPBA), 2. 1,3,5-Trinitrobenzene (TNB), 3. 2,4,6-Trinitrotoluene (TNT)) (addition as solid, series C: 1. m-CPBA, 2. TATP, 3. HMTD)] on suitable diluted solutions of the dye in an organic solvent, usually miscible with water, and the physical changes were followed by fluorescence measurements. Those compounds showing an utmost performance in terms of sensitivity and selectivity to the presence of nitroaromatics were then subjected to TNT/TNB sensitivity in different solvents, and the changes monitored by fluorescence measurements. Then, kinetic behavior and titration experiments were performed, first in different solvents, then by accurate titration in the best solvent, selected from previous experiments. The mechanism of detection was subsequently studied by NMR titration experiments.

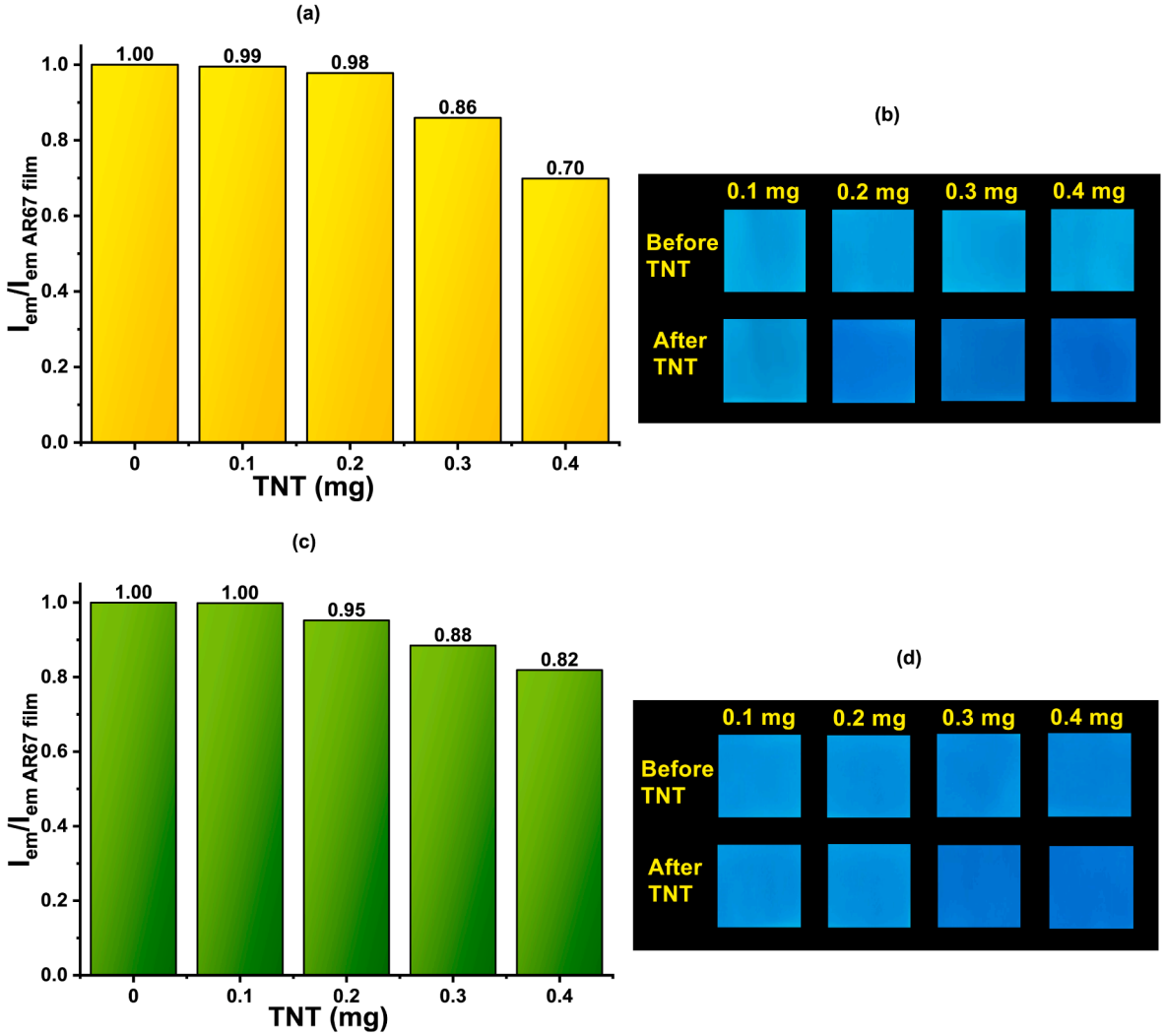

Fig. 16. (a) Variation of the fluorescence emission intensity of the AR67@Sylgard-184 films, before and after contact with increasing amounts of TNT (0, 0.10, 0.20, 0.30 and 0.40 mg) collected from filtered tap water samples. (b) Photographs under 366 nm UV light of AR67@Sylgard-184 films before and after being in contact with increasing amounts of TNT collected from filtered tap water samples. (c) Variation of the fluorescence emission intensity of the AR67@Sylgard-184 films, before and after being placed in contact with increasing amounts of TNT (0, 0.10, 0.20, 0.30 and 0.40 mg) collected from sand. (d) Photographs under 366 nm UV light of AR67@Sylgard-184 films before and after being in contact with increasing amounts of TNT collected from sand.

4. Conclusion

We have described the proof of concept of a portable testing setup for the detection of 2,4,6-trinitrotoluene (TNT), a common component in improvised explosive devices, as well as related explosives such as 1,3,5-trinitrobenzene (TNB), 2,4,6-trinitrophenol (TNP), and explosive taggants such as 2,4-dinitrotoluene (DNT) and nitrobenzene (NB). The system allows for field-testing and generation of real-time results to test for TNT traces on surfaces by simply passing a piece of paper or of the PDMS-supported sensing material on the suspected surface of an ordinary object. In this way, the controlled trapping of the analyte in the paper or chemical sensor gives reliable results for the detection of TNT solid traces under real life conditions. The system may have immediate applications in everyday use. Samples at airports, government buildings, sports arenas, or concert halls, should be checked for IED-containing nitroaromatic explosives to prevent terrorist acts. The system provides for a low limit of detection of traces of TNT on surfaces as it is required to be of practical use. As a complement, we report the preparation of a modified Sylgard film that is useful under real conditions for qualitative fluorescent detection of hidden traces of TNT on surfaces or fingers by a swab method. The combination of quantitative and qualitative detection of TNT traces on surfaces constitutes a comprehensive new method for the detection of hidden nitroaromatic explosives in the workplace. TNT detection as we have shown here is a useful and non-invasive method suitable for explosive detection among current explosive detection technologies to be applied whenever it is necessary for the detection of traces of IEDs, before they can cause any harm.

Funding Sources.

NATO Science for Peace and Security Programme (Grant SPS G5536).

Ministerio de Ciencia e Innovación (Grants PID2019-111215RB-I00 and PDC2022-133955-I00).

Secretaría General de Universidades (FPU18/03225 Grant).

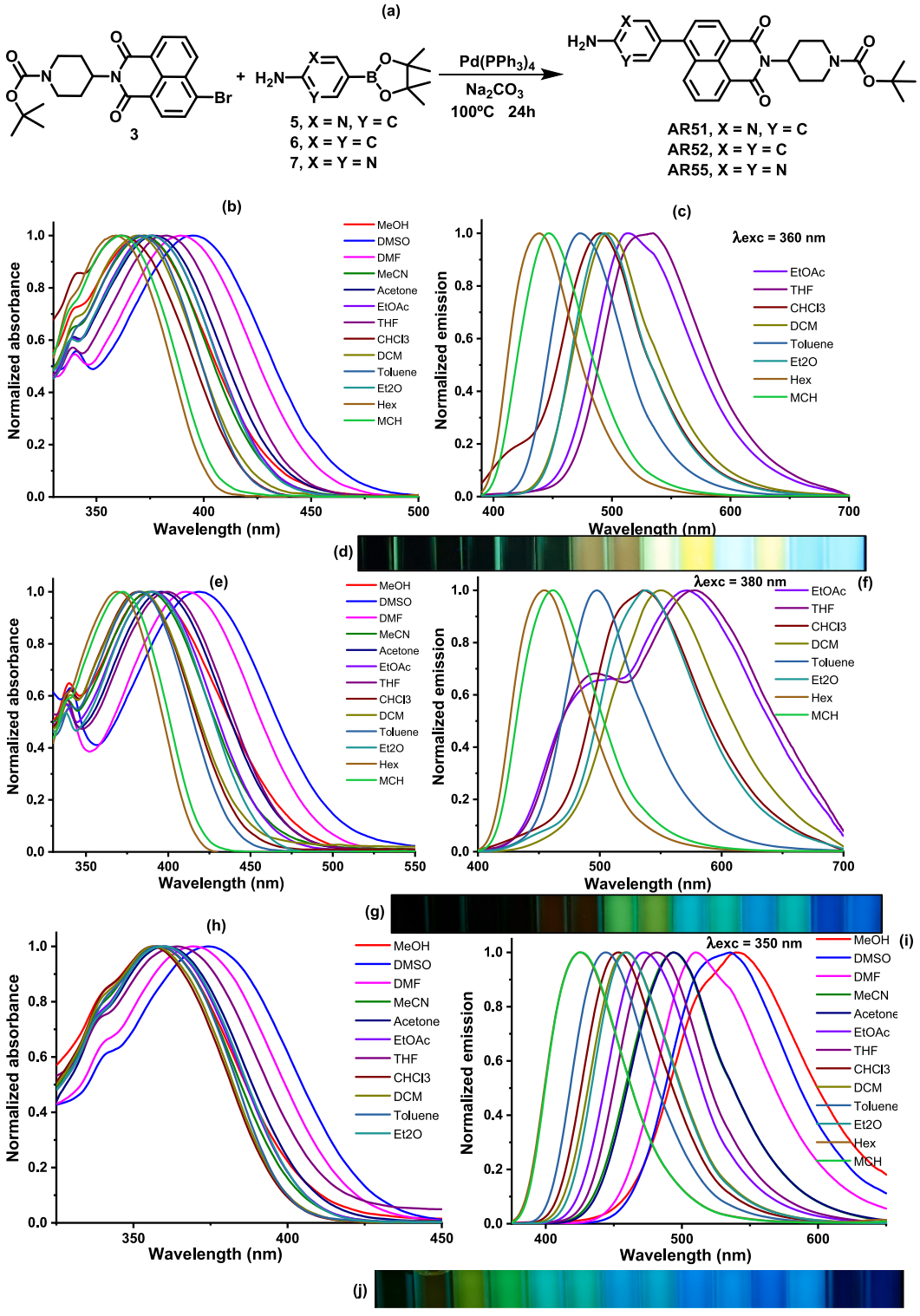

Fig. 17. (a) Synthesis of AR51, AR52 and AR55, (b) AR51 normalized absorbance curves and (c) AR51 fluorescence emission in several solvents, (d) image of the fluorescence of AR51 solutions under UV light, 366 nm, AR51 10 μM in [1] H_2O, [2] MeOH, [3] DMSO, [4] DMF, [5] MeCN, [6] Acetone, [7] EtOAc, [8] THF, [9] $CHCl_3$, [10] CH_2Cl_2, [11] Toluene, [12] Et_2O, [13] Hexane and [14] MCH. (e) AR52 normalized absorbance curves and (f) AR52 fluorescence emission in several solvents, (g) image of the fluorescence of AR52 solutions under UV light, 366 nm, AR52 10 μM in the same list of solvents. (h) AR55 normalized absorbance curves and (i) AR55 fluorescence emission in several solvents, (j) image of the fluorescence of AR55 solutions under UV light, 366 nm, AR55 10 μM in the same list of solvents.

CRediT authorship contribution statement

Andrea Revilla-Cuesta: Investigation, Validation, Formal analysis, Methodology. **Irene Abajo-Cuadrado:** Visualization, Validation, Formal analysis, Methodology. **María Medrano:** Methodology, Investigation, Formal analysis, Data curation. **Mateo M. Salgado:** Investigation, Validation, Methodology. **Giuditta Pecori:** Investigation, Validation, Methodology. **Teresa Rodríguez:** Investigation, Formal analysis, Data curation. **Carla Hernando-Muñoz:** Investigation, Validation, Methodology. **José García-Calvo:** Methodology, Formal analysis, Data curation. **Julia Arcos:** Methodology, Formal analysis, Data curation. **Tomás Torroba:** Conceptualization, Funding acquisition, Writing – original draft, Supervision, Project administration.

Declaration of Competing Interest

The authors declare that they have no known competing financial interests or personal relationships that could have appeared to influence the work reported in this paper.

Data availability

Data will be made available on request.

Acknowledgments

This research was funded by the NATO Science for Peace and Security Programme (Grant SPS G5536) and the Ministerio de Ciencia e Innovación (Grants PID2019-111215RB-I00 and PDC2022-133955-I00). A. R. C. thanks Secretaría General de Universidades for a FPU18/03225 Grant.

Appendix A. Supplementary data

Supplementary data to this article can be found online at https://doi.org/10.1016/j.jphotochem.2023.114911.

References

[1] Improvised Explosive Devices - Past, Present and Future, Action on Armed Violence, 15 Oct 2020, https://reliefweb.int/report/world/improvised-explosive-devices-past-present-and-future, accessed 20/02/2023.
[2] IED Attack, Improvised Explosive Devices, National Academies and the Department of Homeland Security, Dec. 15, 2020, https://www.dhs.gov/xlibrary/assets/prep_ied_fact_sheet.pdf, accessed 20/02/2023.
[3] Reducing the Threat of Improvised Explosive Device Attacks by Restricting Access to Explosive Precursor Chemicals, National Academies of Sciences, Engineering, and Medicine, 2018, The National Academies Press, Washington, DC, https://doi.org/10.17226/24862.
[4] Improvised Explosive Device (IED) Guidelines for Crowded Places, Commonwealth of Australia 2017, ISBN: 978-1-925593-95-2.
[5] United Nations Mine Action Service - Improvised Explosive Device Lexicon, https://unmas.org/sites/default/files/un-mas_ied_lexicon_0.pdf, accessed 20/02/2023.
[6] European Union Terrorism Situation and Trend Report 2019, European Union Agency for Law Enforcement Cooperation, 2019, https://doi.org/10.2813/788404.
[7] K.C. To, S. Ben-Jaber, I.P. Parkin, Recent Developments in the Field of Explosive Trace Detection, ACS Nano 14 (2020) 10804–10833, https://doi.org/10.1021/acsnano.0c01579.
[8] T. Wasilewski, J. Gębicki, W. Kamysz, Bio-inspired approaches for explosives detection, Trends Anal. Chem. 142 (2021), 116330, https://doi.org/10.1016/j.trac.2021.116330.
[9] T.P. Forbes, S.T. Krauss, G. Gillen, Trace detection and chemical analysis of homemade fuel-oxidizer mixture explosives: Emerging challenges and perspectives, Trends Anal. Chem. 131 (2020), 116023, https://doi.org/10.1016/j.trac.2020.116023.
[10] R. Liu, Z. Li, Z. Huang, K. Li, Y. Lv, Biosensors for explosives: State of art and future trends, Trends Anal. Chem. 118 (2019) 123–137, https://doi.org/10.1016/j.trac.2019.05.034.
[11] R. Apak, S.D. Çekiç, A. Uzer, E. Çapanoglu, S.E. Çelik, M. Bener, Z. Can, S. Durmazel, Colorimetric sensors and nanoprobes for characterizing antioxidant and energetic substances, Anal. Methods 12 (2020) 5266–5321, https://doi.org/10.1039/d0ay01521k.
[12] A. Ostrinskaya, R.R. Kunz, M. Clark, R.P. Kingsborough, T.-H. Ong, S. Deneault, Rapid Quantitative Analysis of Multiple Explosive Compound Classes on a Single Instrument via Flow-Injection Analysis Tandem Mass Spectrometry, J. Forensic Sci. 64 (2019) 223–230, https://doi.org/10.1111/1556-4029.13827.
[13] J.M.E. Glackin, R.N. Gillanders, F. Eriksson, M. Fjällgren, J. Engblom, S. Mohammed, I.D.W. Samuel, G.A. Turnbull, Explosives detection by swabbing for improvised explosive devices, Analyst 145 (2020) 7956–7963, https://doi.org/10.1039/D0AN01312A.
[14] T.-H. Ong, T. Mendum, G. Geurtsen, J. Kelley, A. Ostrinskaya, R. Kunz, Use of Mass Spectrometric Vapor Analysis To Improve Canine Explosive Detection Efficiency, Anal. Chem. 89 (2017) 6482–6490, https://doi.org/10.1021/acs.analchem.7b00451.
[15] Z. Li, J.R. Askim, K.S. Suslick, The Optoelectronic Nose: Colorimetric and Fluorometric Sensor Arrays, Chem. Rev. 119 (2019) 231–292, https://doi.org/10.1021/acs.chemrev.8b00226.
[16] J.R. Askim, Z. Li, M.K. LaGasse, J.M. Rankin, K.S. Suslick, An optoelectronic nose for identification of explosives, Chem. Sci. 7 (2016) 199–206, https://doi.org/10.1039/C5SC02632F.
[17] A. V. Kuznetsov, O. I. Osetrov, Detection of Improvised Explosives (IE) and Explosive Devices (IED), In Prediction and Detection of Improvised Explosive Devices (IED), Meeting Proceedings RTO-MP-SET-117, 2007, Paper 14, https://www.sto.nato.int 〉 MP-SET-117-14, accessed 20/02/2023.
[18] C. Ferrari, G. Attolini, M. Bosi, C. Frigeri, P. Frigeri, E. Gombia, L. Lazzarini, F. Rossi, L. Seravalli, G. Trevisi, R. Lolli, L. Aversa, R. Verucchi, N. Musayeva, M. Alizade, S. Quluzade, T. Orujov, F. Sansone, L. Baldini, F. Rispoli, Detection of Nitroaromatic Explosives in Air by Amino-Functionalized Carbon Nanotubes, Nanomaterials 12 (2022) 1278, https://doi.org/10.3390/nano12081278.
[19] D.C. Romero, P. Calvo-Gredilla, J. García-Calvo, A. Diez-Varga, J.V. Cuevas, A. Revilla-Cuesta, N. Busto, I. Abajo, G. Aullón, T. Torroba, Self-Assembly Hydrosoluble Coronenes: A Rich Source of Supramolecular Turn-On Fluorogenic Sensing Materials in Aqueous Media, Org. Lett. 23 (2021) 8727–8732, https://doi.org/10.1021/acs.orglett.1c03175.
[20] S. Kim, H. Kim, T. Qiao, C. Cha, S.K. Lee, K. Lee, H.J. Ro, Y. Kim, W. Lee, H. Lee, Fluorescence Enhancement from Nitro-Compound-Sensitive Bacteria within Spherical Hydrogel Scaffolds, ACS Appl. Mater. Interfaces 11 (2019) 14354–14361, https://doi.org/10.1021/acsami.9b02262.
[21] Z. Zhang, S. Chen, R. Shi, J. Ji, D. Wang, S. Jin, T. Han, C. Zhou, Q. Shu, A single molecular fluorescent probe for selective and sensitive detection of nitroaromatic explosives: A new strategy for the mask-free discrimination of TNT and TNP within same sample, Talanta 166 (2017) 228–233, https://doi.org/10.1016/j.talanta.2017.01.046.
[22] N. Tripathi, R. Kumar, P. Singh, S. Kumar, Ratiometric fluorescence "Turn On" probe for fast and selective detection of TNT in solution, solid and vapour, Sens. Actuators B Chem 246 (2017) 1001–1010, https://doi.org/10.1016/j.snb.2017.02.174.
[23] J.Y. Lee, H.D. Root, R. Ali, W. An, V.M. Lynch, S. Bähring, I.S. Kim, J.L. Sessler, J. S. Park, Ratiometric Turn-On Fluorophore Displacement Ensembles for Nitroaromatic Explosives Detection, J. Am. Chem. Soc. 142 (2020) 19579–19587, https://doi.org/10.1021/jacs.0c08106.
[24] M. Bener, F.B. Sen, R. Apak, Protamine gold nanoclusters - based fluorescence turn-on sensor for rapid determination of Trinitrotoluene (TNT), Spectrochim. Acta A: Mol. Biomol. Spectrosc. 279 (2022), 121462, https://doi.org/10.1016/j.saa.2022.121462.
[25] H.M. Junaid, M.T. Waseem, Z.A. Khan, H. Gul, C. Yu, A.J. Shaikh, S.A. Shahzad, Fluorescent and colorimetric sensors for selective detection of TNT and TNP explosives in aqueous medium through fluorescence emission enhancement mechanism, J. Photochem. Photobiol. A: Chem. 428 (2022), 113865, https://doi.org/10.1016/j.jphotochem.2022.113865.
[26] W.-M. Wan, D. Tian, Y.-N. Jing, X.-Y. Zhang, W. Wu, H. Ren, H.-L. Bao, NBN-Doped Conjugated Polycyclic Aromatic Hydrocarbons as an AIEgen Class for Extremely Sensitive Detection of Explosives, Angew. Chem. Int. Ed. 57 (2018) 15510–15516, https://doi.org/10.1002/anie.201809844.
[27] K.K. Kartha, S.S. Babu, S. Srinivasan, A. Ajayaghosh, Attogram Sensing of Trinitrotoluene with a Self-Assembled Molecular Gelator, J. Am. Chem. Soc. 134 (2012) 4834–4841, https://doi.org/10.1021/ja210728c.
[28] A.S. Tanwar, R. Parui, R. Garai, M.A. Chanu, P.K. Iyer, Dual "Static and Dynamic" Fluorescence Quenching Mechanisms Based Detection of TNT via a Cationic Conjugated Polymer, ACS Meas. Sci. Au 2 (2022) 23–30, https://doi.org/10.1021/acsmeasuresciau.1c00023.
[29] X.-S. Ma, Y.-Z. Cui, Y.-Q. Ding, F.-R. Tao, B. Zheng, R.-H. Yu, W. Huang, 2D hyperbranched conjugated polymer for detecting TNT with excellent exciton migration, Sens. Actuators B Chem. 238 (2017) 48–57, https://doi.org/10.1016/j.snb.2016.07.025.
[30] H. Nie, Y. Lv, L. Yao, Y. Pan, Y. Zhao, P. Li, G. Sun, Y. Ma, M. Zhang, Fluorescence detection of trace TNT by novel cross-linking electropolymerized films both in vapor and aqueous medium, J. Hazard. Mater. 264 (2014) 474–480, https://doi.org/10.1016/j.jhazmat.2013.09.031.
[31] B. Zhu, L. Zhu, Y. Wan, S. Deng, C. Zhang, J. Luo, Multicomponent metal-organic frameworks with aggregation-induced emission characteristics as fluorescence sensor array for the identification of energetic compounds, Sens. Actuators B Chem. 341 (2021), 130011, https://doi.org/10.1016/j.snb.2021.130011.
[32] H. Zhou, X. Wang, T.T. Lin, J. Song, B.Z. Tang, J. Xu, Poly(triphenyl ethene) and poly(tetraphenyl ethene): synthesis, aggregation-induced emission property and application as paper sensors for effective nitro-compounds detection, Polym. Chem. 7 (2016) 6309–6317, https://doi.org/10.1039/c6py01358a.

[33] M. Chakraborty, B. Prusti, M. Chakravarty, Small Electron-Rich Isomeric Solid-State Emitters with Variation in Coplanarity and Molecular Packings: Rapid and Ultralow Recognition of TNT, ACS Appl. Electron. Mater. 4 (2022) 2481–2489, https://doi.org/10.1021/acsaelm.2c00241.
[34] S. Yadav, N. Choudhary, M.R. Dash, A.R. Paital, High surface area dendritic silica pairing with anthraquinone derivative: A promising single platform for dual applications of detection and remediation of nitroaromatics and copper ion, Chem. Eng. J. 450 (2022), 138042, https://doi.org/10.1016/j.cej.2022.138042.
[35] X. Yu, S. Wan, W. Wu, C. Yang, W. Lu, c-Cyclodextrin-based [2]rotaxane stoppered with gold(I)–ethynyl complexation: phosphorescent sensing for nitroaromatics, Chem. Commun. 58 (2022) 6284–6287, https://doi.org/10.1039/d2cc02256g.
[36] W. Lu, S.A. Asher, Z. Meng, Z. Yan, M. Xue, L. Qiu, D. Yi, Visual detection of 2,4,6-trinitrotolune by molecularly imprinted colloidal array photonic crystal, J. Hazard. Mater. 316 (2016) 87–93, https://doi.org/10.1016/j.jhazmat.2016.05.022.
[37] V. Bhalla, S. Pramanik, M. Kumar, Cyanide modulated fluorescent supramolecular assembly of a hexaphenylbenzene derivative for detection of trinitrotoluene at the attogram level, Chem. Commun. 49 (2013) 895–897, https://doi.org/10.1039/c2cc36872b.
[38] M. Paul, G. Tscheuschner, S. Herrmann, M.G. Weller, Fast Detection of 2,4,6-Trinitrotoluene (TNT) at ppt Level by a Laser-Induced Immunofluorometric Biosensor, Biosensors 10 (2020) 89, https://doi.org/10.3390/bios10080089.
[39] T. Komikawa, M. Tanaka, K. Yanai, B.R.G. Johnson, K. Critchley, T. Onodera, S. D. Evans, K. Toko, M. Okochi, A bioinspired peptide matrix for the detection of 2,4,6-trinitrotoluene (TNT), Biosens. Bioelectron. 153 (2020), 112030, https://doi.org/10.1016/j.bios.2020.112030.
[40] H. Bai, G. Wen, A. Liang, Z. Jiang, Ti3C2@Pd nanocatalytic amplification-polypeptide SERS/RRS/Abs trimode biosensoring platformfor ultratrace trinitrotoluene, Biosens. Bioelectron. 217 (2022), 114743, https://doi.org/10.1016/j.bios.2022.114743.
[41] S. Tang, N. Vinerot, D. Fisher, V. Bulatov, Y. Yavetz-Chen, I. Schechter, Detection and mapping of trace explosives on surfaces under ambient conditions using multiphoton electron extraction spectroscopy (MEES), Talanta 155 (2016) 235–244, https://doi.org/10.1016/j.talanta.2016.04.027.
[42] A. Lichtenstein, E. Havivi, R. Shacham, E. Hahamy, R. Leibovich, A. Pevzner, V. Krivitsky, G. Davivi, I. Presman, R. Elnathan, Y. Engel, E. Flaxer, F. Patolsky, Supersensitive fingerprinting of explosives by chemically modified nanosensors arrays, Nat. Commun. 5 (2014) 4195, https://doi.org/10.1038/ncomms5195.
[43] A. González-Calabuig, X. Cetó, M. del Valle, Electronic tongue for nitro and peroxide explosive sensing, Talanta 153 (2016) 340–346, https://doi.org/10.1016/j.talanta.2016.03.009.
[44] X. Sun, Y. Wang, Y. Lei, Fluorescence based explosive detection: from mechanisms to sensory materials, Chem. Soc. Rev. 44 (2015) 8019–8061, https://doi.org/10.1039/C5CS00496A.
[45] P. Calvo-Gredilla, J. García-Calvo, J.V. Cuevas, T. Torroba, J.-L. Pablos, F. C. García, J.-M. García, N. Zink-Lorre, E. Font-Sanchis, A. Sastre-Santos, F. Fernández-Lázaro, Solvent-Free Off–On Detection of the Improvised Explosive Triacetone Triperoxide (TATP) with Fluorogenic Materials, Chem. Eur. J. 23 (2017) 13973–13979, https://doi.org/10.1002/chem.201702412.
[46] J. García-Calvo, P. Calvo-Gredilla, M. Ibáñez-Llorente, D.C. Romero, J.V. Cuevas, G. García-Herbosa, M. Avella, T. Torroba, Surface functionalized silica nanoparticles for the off–on fluorogenic detection of an improvised explosive, TATP, in a vapour flow, J. Mater. Chem. A 6 (2018) 4416–4423, https://doi.org/10.1039/C7TA10792G.
[47] S. Blanco, A. Macario, J. García-Calvo, A. Revilla-Cuesta, T. Torroba, J.C. López, Microwave Detection of Wet Triacetone Triperoxide (TATP): Non-Covalent Forces and Water Dynamics, Chem. Eur. J. 27 (2021) 1680–1687, https://doi.org/10.1002/chem.202003499.
[48] S. Lapcinska, A. Revilla-Cuesta, I. Abajo-Cuadrado, J.V. Cuevas, M. Avella, P. Arsenyan, T. Torroba, Dye-modified silica-anatase nanoparticles for the ultrasensitive fluorogenic detection of the improvised explosive TATP in an air microfluidic device, Mater. Chem. Front. 5 (2021) 8097–8107, https://doi.org/10.1039/D1QM01041G.
[49] P. Gopikrishna, N. Meher, P.K. Iyer, Functional 1,8-Naphthalimide AIE/AIEEgens: Recent Advances and Prospects, ACS Appl. Mater. Interfaces 10 (2018) 12081–12111, https://doi.org/10.1021/acsami.7b14473.
[50] K. Tajima, N. Fukui, H. Shinokubo, Aggregation-Induced Emission of Nitrogen-Bridged Naphthalene Monoimide Dimers, Org. Lett. 21 (2019) 9516–9520, https://doi.org/10.1021/acs.orglett.9b03699.
[51] Y. Wang, Y. Teng, H. Yang, X. Li, D. Yin, Y. Tian, Bioorthogonally applicable multicolor fluorogenic naphthalimide–tetrazine probes with aggregation-induced emission characters, Chem. Commun. 58 (2022) 949–952, https://doi.org/10.1039/D1CC05204G.
[52] H. Ma, C. He, X. Li, O. Ablikim, S. Zhang, M. Zhang, A fluorescent probe for TNP detection in aqueous solution based on joint properties of intramolecular charge transfer and aggregation-induced enhanced emission, Sens. Actuators B Chem. 230 (2016) 746–752, https://doi.org/10.1016/j.snb.2016.02.112.
[53] X. Jiao, H. Li, X. Cheng, Cellulose-based fluorescent macromolecular sensors and their ability in 2,4,6-trinitrophenol detection, Mater. Today Chem. 22 (2021), 100615, https://doi.org/10.1016/j.mtchem.2021.100615.
[54] B. Díaz de Greñu, D. Moreno, T. Torroba, A. Berg, J. Gunnars, T. Nilsson, R. Nyman, M. Persson, J. Pettersson, I. Eklind, P. Wästerby, Fluorescent Discrimination between Traces of Chemical Warfare Agents and Their Mimics, J. Am. Chem. Soc. 136 (2014) 4125–4128, https://doi.org/10.1021/ja500710m.
[55] B. Díaz de Greñu, J. García-Calvo, J. Cuevas, G. García-Herbosa, B. García, N. Busto, S. Ibeas, T. Torroba, B. Torroba, A. Herrera, S. Pons, Chemical speciation of MeHg+ and Hg2+ in aqueous solution and HEK cells nuclei by means of DNA interacting fluorogenic probes, Chem. Sci. 6 (2015) 3757–3764, https://doi.org/10.1039/C5SC00718F.
[56] J. García-Calvo, S. Vallejos, F.C. García, J. Rojo, J.M. García, T. Torroba, A smart material for the in situ detection of mercury in fish, Chem. Commun. 52 (2016) 11915–11918, https://doi.org/10.1039/C6CC05977E.
[57] J. García-Calvo, P. Calvo-Gredilla, M. Ibáñez-Llorente, T. Rodríguez, T. Torroba, Detection of Contaminants of High Environmental Impact by Means of Fluorogenic Probes, Chem. Rec. 16 (2016) 810–824, https://doi.org/10.1002/tcr.201500253.
[58] J. García-Calvo, J.A. Robson, T. Torroba, J.D.E.T. Wilton-Ely, Synthesis and Application of Ruthenium(II) Alkenyl Complexes with Perylene Fluorophores for the Detection of Toxic Vapours and Gases, Chem. Eur. J. 25 (2019) 14214–14222, https://doi.org/10.1002/chem.201903303.
[59] V. García-Calvo, J.V. Cuevas, H. Barbero, S. Ferrero, C.M. Álvarez, J.A. González, B. Díaz de Greñu, J. García-Calvo, T. Torroba, Synthesis of a Tetracorannulene-perylenediimide That Acts as a Selective Receptor for C60 over C70, Org. Lett. 21 (2019) 5803–5807, https://doi.org/10.1021/acs.orglett.9b01729.
[60] N. Busto, P. Calvo, J. Santolaya, J.M. Leal, A. Guédin, G. Barone, T. Torroba, J.-L. Mergny, B. García, Fishing for G-Quadruplexes in Solution with a Perylene Diimide Derivative Labeled with Biotins, Chem. Eur. J. 24 (2018) 11292–11296, https://doi.org/10.1002/chem.201802365.
[61] J. García-Calvo, T. Torroba, V. Brañas-Fresnillo, G. Perdomo, I. Cózar-Castellano, Y.-H. Li, Y.-M. Legrand, M. Barboiu, Manipulation of Transmembrane Transport by Synthetic K+ Ionophore Depsipeptides and Its Implications in Glucose-Stimulated Insulin Secretion in β-Cells, Chem. Eur. J. 25 (2019) 9287–9294, https://doi.org/10.1002/chem.201901372.
[62] N. Busto, J. García-Calvo, J.V. Cuevas, A. Herrera, J.-L. Mergny, S. Pons, T. Torroba, B. García, Influence of core extension and side chain nature in targeting G-quadruplex structures with perylene monoimide derivatives, Bioorg. Chem. 108 (2021), 104660.
[63] J. García-Calvo, P. Calvo-Gredilla, S. Vallejos, J.M. García, J.V. Cuevas-Vicario, G. García-Herbosa, M. Avella, T. Torroba, Palladium nanodendrites uniformly deposited on the surface of polymers as an efficient and recyclable catalyst for direct drug modification via Z-selective semihydrogenation of alkynes, Green Chem. 20 (2018) 3875–3883, https://doi.org/10.1039/C8GC01522H.
[64] J. García-Calvo, V. García-Calvo, S. Vallejos, F.C. García, M. Avella, J.-M. García, T. Torroba, Surface Coating by Gold Nanoparticles on Functional Polymers: On-Demand Portable Catalysts for Suzuki Reactions, ACS Appl. Mater. Interfaces 8 (2016) 24999–25004, https://doi.org/10.1021/acsami.6b07746.
[65] C.A. Latendresse, S.C. Fernandes, S. You, H.Q. Zhang, W.B. Euler, Fluorescent Species Formed by Reaction of Trinitroaromatics with N, N-Dimethylformamide and Hydroxide, J. Phys. Chem. A 117 (2013) 324–332, https://doi.org/10.1021/jp309709h.
[66] F. Allegrini, A.C. Olivieri, IUPAC-Consistent Approach to the Limit of Detection in Partial Least-Squares Calibration, Anal. Chem. 86 (2014) 7858–7866, https://doi.org/10.1021/ac501786u.
[67] M.C. Ortiz, L.A. Sarabia, M.S. Sánchez, Tutorial on evaluation of type I and type II errors in chemical analyses: From the analytical detection to authentication of products and process control, Anal. Chim. Acta. 674 (2010) 123–142, https://doi.org/10.1016/j.aca.2010.06.026.
[68] RStudio, Version 1.4.1103, 2009-2021 RStudio, 250 Northern Ave, Boston, MA 02210.
[69] X. Chen, X. Zhang, H. Wang, L. Zhang, J. Zhu, Trace Explosive Detection Based on Photonic Crystal Amplified Fluorescence, Chem. Eur. J. (2023) e202203605.
[70] K.L. Hutchinson, D.M. Stoltzfus, P.L. Burn, P.E. Shaw, Luminescent poly (dendrimer)s for the detection of explosives, Mater. Adv. 1 (2020) 837–844, https://doi.org/10.1039/d0ma00249f.
[71] D. Maji, S.K. Lahiri, S. Das, Study of hydrophilicity and stability of chemically modified PDMS surface using piranha and KOH solution, Surf. Interface Anal. 44 (2012) 62–69, https://doi.org/10.1002/sia.3770.